

Final Report
on
RESEARCH PROJECT 105:
FULL-SCALE EXPERIMENTAL INVESTIGATION
OF THE STRUCTURAL RESPONSE OF THE
BONNERS FERRY BRIDGE
by

Principal Investigator: Dr. Donald F. Haber, Dr. Dale C. Perry
(208) 885-6405
Research Engineers: Thomas A. Hubbell
Jeffrey T. Hubbell
Matthew Schaller
George Inverso

Prepared for the Idaho Transportation Department

Department of Civil Engineering
University of Idaho

Final Report
on
RESEARCH PROJECT 105:
FULL-SCALE EXPERIMENTAL INVESTIGATION
OF THE STRUCTURAL RESPONSE OF THE
BONNERS FERRY BRIDGE

by

Principal Investigator: Dr. Donald F. Haber, Dr. Dale C. Perry
(208) 885-6405
Research Engineers: Thomas A. Hubbell
Jeffrey T. Hubbell
Matthew Schaller
George Inverso

Prepared for the Idaho Transportation Department

Department of Civil Engineering
University of Idaho

Acknowledgements

This report and all field work was made possible by financial support from the Idaho Transportation Department. The opinions, findings and conclusions expressed in this publication are those of the authors and not necessarily those of the Idaho Transportation Department or T. Y. Lin International, the bridge designers.

The authors would also like to acknowledge the following persons whose help was essential to the completion of this work:

Idaho Transportation Department -

Mr. James Hill, Research Supervisor

Mr. R. A. Jobes, Bridge Design Supervisor

Mr. James W. Richard, Group Leader, Bridge Section

Mr. Sid Scribner, Resident Engineer, Sandpoint

Mr. Tom Jee of T. Y. Lin International and those involved with the construction of the girders and bridge from Peter Kewitt & Sons, and Robberson Steel Company.

TABLE OF CONTENTS

A. Report

	Page Number
I. Introduction.....	1
II. Objectives.....	3
III. Design Criteria.....	4
IV. General Superstructure Details.....	6
V. Construction Sequence.....	7
VI. Field Study.....	9
VII. Finite Element Analysis.....	12
VIII. Live Load Field Test Procedure.....	14
IX. Test Discussion.....	15
X. Summary and Recommendations.....	21

B. Tables

1-4.....	23-26
----------	-------

C. Figures

1-46.....	27-72
-----------	-------

INTRODUCTION

The new Bonners Ferry bridge is a 1378 foot steel bridge on U.S. 95 over the Kootenai River and the Spokane International Railroad located at Bonners Ferry in Boundary County, Idaho. The bridge has nine reinforced concrete piers spanned by four post-tensioned welded steel plate girders topped by a reinforced prestressed concrete deck.

Construction on the bridge started in the spring of 1983 and was essentially completed by the fall of 1984 and opened to full traffic on June 23, 1985. The bridge was designed by the Firm of T. Y. Lin International, (TYLI) for the State of Idaho Transportation Department. After the final design was completed and before construction was started in the spring of 1983, the Idaho Transportation Department contracted with the University of Idaho to conduct field strain measurements and an analytical investigation of the structural response of the new bridge. The research study for this bridge was undertaken because of the unique design which incorporated for the first time the use of post-tensioned steel plate girders.

The field work was started in the spring of 1984 and strain gages were installed at critical locations on the steel girders and in the concrete deck as determined by the University investigators. The gages were installed on the girders prior to post-tensioning and in the deck on reinforcing before concrete placement. Measurements of the strains were recorded at critical construction events through the entire construction period including post construction live load test strain measurements.

A finite element type computer algorithm was used in the analytical investigation. This allowed a comparison between field, design and

analytically determined dead load and live load static structural response.

OBJECTIVES:

The objectives of this investigation were as follows:

Prior to Construction:

- 1) Compute the anticipated axial and bending stresses present in various members for several stages of loading at points where instrumentation were to be installed using the design theory and assumptions established by the finite element program, and T. Y. Lin, International.
- 2) Design, purchase, assemble, calibrate and test the monitoring system at the University of Idaho Laboratory.

During Construction:

- 1) Monitor the girder post-tension stresses and tendon force at the stressing of the tendons for the location on the bridge.
- 2) Install monitoring system as construction progresses.
- 3) Record field data for each stage of construction loading.

After Construction:

- 1) Record field data for a test truck provided by the Department.
- 2) Compile all field data and evaluate results.
- 3) Compare the results in the field study structural response with the original design response and the response determined by finite element techniques.

DESIGN CRITERIA:

The bridge structure was designed in accordance with 1977 AASHTO Specifications and 1978 & 1979 Interim Specifications using Load Factor and Service Load design.

Live Load: HS25 = (1.25)HS20 (1.44 lane/girder)

Wearing Surface: 22 psf (16 psf future)

Utilities: 100 plf

Pile Capacity: 90 tons per pile

Footing Capacity: 20 TSF

Seismic Capacity: Max. bed rock acceleration = 0.07g

Wind Velocity: 80 mph

Stream Velocity: 2.4 fps

Thermal: -75° + 50°F (Normal at 65°F)

Earth Pressure: Equivalent fluid pressure = 35 pcf

Surcharge (HS25) = 2.5 ft.

Material

Structural Steel: ASTM-A588 fy=50,000 psi

Steel Fasteners: ASTM-A325-Type 3

Prestressing Steel: ASTM-A416 Strand $f_s' = 270$ ksi

Pedestrian Rail (Aluminum) ASTM-B221

Concrete

Substructure: $f_c' = 4,000$ psi (Cap and Column)

$f_c' = 3,000$ psi (Abutment and Footing)

Unit Weight = 150 pcf

Deck Slab: $f_c' = 5,000$ psi

Unit Weight = 150 pcf

Reinforcing steel: Grade 60 fy = 60,000 psi

Construction Specification: Construction was done in accordance with
Idaho Transportation Department Division of Highway Standard
Specifications 1976 Edition and Supplemental Specifications

GENERAL SUPERSTRUCTURE DETAILS.

The superstructure consists of four steel girder lines (A, B, C, D) supporting a transverse post-tensioned composite concrete slab with a four-lane roadway, shoulders, traffic parapet railing, a pedestrian walkway and city water line. Center-to-center girder spacing varies from 18' - 0" in the tangent section of the bridge to nearly 23' in the curved portions of the bridge near the abutments. (See Fig. 1) Longitudinally, the span lengths vary from 100' - 0" at the north abutment to 155' -0" at the main river spans. Field splices located 32' from each pier result in actual girder segment lengths from 64 ft for pier segments to 91 feet for drop-in segments. (See Figures 2, 3, 4, 5, 6).

Post-Tension Details

Stage I Pre-Stressing tendons were attached to the steel girder top flanges of the 64' pier girder segments at piers 1 through 7 to counteract the effects of dead and live loads and provide adequate negative moment resistance with smaller flange plates. Additional longitudinal post-tensioning tendons were placed in the deck over the piers to pre-stress the deck. This additional prestressing was to offset tension induced into the deck by negative moment live loads. The deck throughout is connected to the top flange with shear connectors. (See Figures 7 - 11). The pre-stressing allows a reduction in flange plate area for economy.

CONSTRUCTION SEQUENCE

Fabrication of the girders was performed by Robberson Steel Company in Oklahoma City, Oklahoma. The project specifications required a progressive shop assembly for all girders. This required temporary stressing of the pier segments in the shop. Since the temporary stressing of the girders would have been time consuming and costly, the fabricator proposed a blocking system to simulate the deflected position of the girder. Girder deflections were verified by shop stressing two girders. After successful completion of this test, the fabricator's blocking and assembly procedure, without stressing of the pier segments, was approved.

After fabrication, the girders were shipped to the site by rail. Once delivered to the jobsite, the girders were erected starting at the north abutment and proceeding southward (Fig. 12). Pairs of the pier girder segments were placed in position for assembly at a staging site just upstream from the north abutment. After all cross frames between the two girders were installed (Figs. 5, 6), a temporary timber work platform was placed on the lower girder flanges. The post-tensioning anchor assemblies were attached to the top flanges plastic ducts placed between them, and the tendons installed and stressed (See Fig. 9, Table 1). All tendon ducts were then filled with grout and the units remained on the ground until grout strengths achieved specified levels (usually 7 days). The girder pairs were then placed on a barge for transport to the proper pier locations. Once in place on the piers, the pair of girder segments were supported by cable stays down to the pier shafts and the remaining interior bay cross framing was installed. The 91 foot drop-in spans were then lifted one at a time into position and bolted

field splices were completed. Figure 12 shows the erection sequence for the north portion of the bridge.

Once complete spans were erected, deck forms were placed and additional longitudinal post-tensioning ducts installed in the deck over the piers (Fig. 10). Transverse to the centerline of the bridge, 4 strand tendons at 1'-11" to 2'-6" centers were installed along with mild steel temperature mats in both directions (Fig. 5, 6, 9, 11). Deck concrete was then placed in specified sequences to control deflections of the girders (Fig. 12). Blockouts at tendon anchorages were left so tensioning jacks could operate. When concrete strengths reached 3500 psi, longitudinal and transverse tendons were stressed. Parapet railing placement followed the deck placement across the bridge.

Due to some surface irregularities in the deck and the large number of blockouts for post-tensioning, a decision was made to place an latex-concrete overlay immediately instead of the asphalt cement wearing surface originally planned for the future. The top $\frac{1}{4}$ " of the deck was removed, the surface sandblasted and a $1\frac{1}{2}'' \pm$ thick latex-modified concrete overlay placed in August 1984. Due to incomplete paving of the approach roadway, the structure was then opened to limited traffic in September 1984. The paving was completed and the bridge opened to full service on June 27, 1985.

FIELD STUDY

Installation of Permanent Structural Response Instrumentation

The first 13 months of this research project was devoted to the selection, calibration and installation of the necessary transducers to monitor the structural response of the bridge. As depicted in Figs. 13-17, extensive clusters of strain gages and thermocouples were installed at four locations, 1^a through 4^a. Locations 1^a and 3^a were chosen to monitor girder and deck stresses in negative moment regions - one in which cable stressing of the girders was introduced (over Pier 5 Fig. 14)) and one without cable stressing (over Pier 8 (Fig. 16). Location 2^a is located at mid-span between Piers 5 and 6 in a positive moment region (Fig. 15).

During the construction of the deck over Pier 8, a breakdown in communication occurred between the principal investigator and the contractor. As a result, the concrete was placed prior to installation of the deck strain and temperature gages originally contemplated at this location. Subsequently, the State requested that instrumentation be provided over Pier 7 (location 4^a Fig. 17).

All of the strain gages and temperature sensors installed were of the "weldable type." Additionally, although these gages were hermetically sealed by the manufacturer, the same type of waterproofing normally employed for epoxy gages was used throughout so as to provide maximum gage life (estimated at between 7-10 years). All transducer cable runs are continuous between the gage location and the instrumentation shack and are protected by PVC conduit throughout.

Monitoring of Cable Stressing of Girders

To evaluate the influence of cable stressing on girders C and D erected over Pier 5, load rings were designed, fabricated and installed at the dead end of each of the tendons A, B and C for the two girders. The load rings consisted essentially of two inch lengths of high strength circular tubing to which 6 strain gages had been attached. The load cells were "exercised" and then calibrated "on-line" with the VSL hydraulic ram to be used in the post-tensioning operation employing the University's MTS loading system. The load cells were shown to be accurate to within 1% of the service tendon prestressing force for a maximum eccentricity of 0.5 in.

The monitored prestressing force in each of the tendons is given in Table 1. The stresses induced in the girders are given in Table 2 under column headed by 9/14 and in Figs. 18 & 19. The values shown in Table 1 correspond to the tendon forces with the girders located at the staging site at the north abutment. Following erection of the girders on the piers and placement of the "drop-in" girders, an attempt was made to reconnect the load rings to the data acquisition system and measure the tendon forces. This attempt proved futile, however, as the load cells had apparently been damaged during the erection process.

Calibration of VSL Hydraulic Ram

In the course of the calibration of the load cells referred to above, it was noted that the VSL gage calibration curve provided for the hydraulic ram did not agree with that obtained from the MTS loading data. To resolve the issue, the State requested that the investigator

obtain an independent confirmation. This was accomplished at the Washington Department of Transportation Testing Laboratory located in Spokane. The results of this series of tests agreed closely with that obtained from the University's MTS system data.

Development of Computer Programs

To gather, process and analyze the data from the 82 channels, an HP 3054 DL Data Logger coupled with an HP 85F Computer was utilized. The appropriate software was developed such that the signals generated from each transducer was processed "on-line" and the corresponding stresses and temperatures induced for each location printed out.

Tabulated Time-History of Stresses

With the exception of the gages located at Pier 7 (Fig. 17), all instrumentation on the girders was installed and zeroed prior to erection. Thus, the stresses given in Table 2 (except for gages at Pier 7) represent a true time-history referenced to the "non-stressed condition." The deck strain and temperature gages were placed and zeroed just prior to the placement of the concrete. Table 3 provides a tabulated time-history of the stresses induced.

Readings were taken periodically during the construction of the bridge as dictated by the construction sequence. See Fig. 12 and Table 2 for the status of construction at the time the readings were taken and stresses computed. The time-history plots with design stresses and computer generated stresses are shown in Figs. 18-25. In addition, live load influence type diagrams generated from readings taken on July 24, 1985 are shown in Figs. 28-44.

FINITE ELEMENT ANALYSIS OF BRIDGE STRUCTURAL RESPONSE

In order to analyze the bridge structural response a finite element program developed at The University of California, Berkeley for static and dynamic analysis of a varied type of structures was utilized. The program is called S.A.P. IV (Structural Analysis Program IV). The data input consists of: 1) general structure geometry, 2) structural member types, 3) member material types, 4) material properties, 5) member geometry, 6) support conditions, and 7) loading conditions.

The general structure geometry of the bridge input was as follows:

Length - 1387 ft

Width - 70 ft (ave.)

No. of nodes - 266

No. of member types - 20

No. of materials - 2 (steel & concrete)

No. of beam elements - 244

Load conditions - 11

The length was divided into 62 unequal parts roughly corresponding to changes in cross section or in sectional properties. (See bridge flange and web diagram Figs. 2, 3, 4). Element lengths varied from 16 ft to 20 ft. The structure was divided longitudinally along the four girder center lines to better analyze the effects of varied width, skewed supports, and a curved roadway, rather than a single center line analysis.

Each girder line was divided into 61 beam elements. These 61 elements consisted of a combination of the 20 member types defined by changes in geometry and materials as the bridge construction progressed.

The first type being steel girders alone, and the last being a composite section composed of the steel girder and concrete deck (see Table 4).

Specific loadings considered were dead weight loads, including false work and loads due to prestressing of both the steel girders and the concrete deck. The gravity loads were input as fixed end forces (11 types), and the prestressing forces were input as point loads at the stressing heads. Due to the S.A.P. IV program's lack of non-linear shear deformation capability, shear effects caused in the steel girders by the prestressing were neglected.

The program was run on the University of Idaho's IBM computer. Basically, the program solves the matrix equation

$$KU = R - R^F$$

where K is the stiffness matrix, U is the displacement matrix, R is the generalized load matrix and R^F is the fixed end force matrix. The bridge stress determination required solving 1,376 linear simultaneous equations. The results of the analytical investigation are summarized in Table 4 and in time-history graphs Figs. 18 - 25.

It should be noted that the program used would not allow the girder prestressing to be input directly. Superposition was used to get the values at piers 1-6.

LIVE LOAD FIELD TEST PROCEDURE

On July 24, 1985, a live load type test was conducted on the bridge using an Idaho Transportation Department two axle truck coupled to a flat-bed trailer. The trailer was loaded with concrete guard rails which produced the axle loadings as shown in Figure 27.

A "no load" test was conducted at the beginning of the test, that is, no vehicles were on the bridge when measurement of all strain gages were recorded. This "no load" test was also conducted at the completion of the load test for each girder.

The truck trailer was then positioned so the front axle was located at station 727.56 with the truck trailer center line five feet from the bridge parapet (Figure 27). Readings were taken for this position. The truck was then advanced 20 ft. until the front axle was located at station 707.56 with the truck center line still five feet from bridge parapet. Readings were taken for this position. This procedure was repeated every 20 ft. until the front axle was at station 147.56. The exact same procedure was used for girder C except the truck was positioned farther from the bridge parapet.

All recorded strain measurements from this live load test were used to calculate induced stresses which determined the influence lines for live load test as shown and discussed in the test discussion section.

TEST DISCUSSION

General Methodology

Three methods were used to determine critical girder stresses. First, the design stresses as determined by T. Y. Lin, International, second, finite element stresses as determined by a computer program (S.A.P. IV) and thirdly, by actual field measurements using strain gages at critical stress locations. For the first two procedures, estimates for the structural properties of the materials, loading conditions, modulus and simplification of the geometric configuration had to be made. The accuracy of these estimates and simplifications will be reflected in the over-all accuracy of predicting "actual" in-situ stresses.

For the field determined stresses, instrument accuracy, experimental error and environmental conditions contribute to the differences between "actual" and measured strain. Thus, reasonable agreement between the stresses determined by three independent methods would indicate the "actual" in-situ stresses are in the same range of values.

Non-prestressed Girders

Analysis of the stress time-history graphs for girders C and D over pier 8 (Figs. 24 - 25) and for span 5-6, girders C and D (Figs. 18-19) indicates excellent agreement between the three methods. For the girders over pier 8 (which are not post-tensioned) there is no noticeable trend in the slight differences between the methods.

For the mid-span girders, girders C and D span 5-6, the design calculated flange stresses seem to consistently overestimate the field determined stresses for the bottom flange. While the finite element method generally underestimates the field stresses for the top flange.

These differences could be attributed to the necessary estimates of load distribution parameters and section properties used in the non-field methods. However, the field determined stresses for these girders are well within design determined stresses, and show excellent agreement with theoretical values.

Post-Tensioned Girders

As previously stated, one of the unique features of this bridge is the use of post-tensioned steel plate girders in the negative moment areas over piers 1-7. For the prestressed girders C and D over pier 5, (Figs. 20,21) considerable differences were found between calculated and field measured stresses during prestressing, and continuing until the dead weight of the concrete deck reduced the compressive stresses in the top flange. (Fig. 18, 19 March, 1984). From that point on we continue to see higher compressive values in the top flange than predicted. Design live loads combined with dead loads should produce tensile readings in the top flange, but field measurement indicates compression.

The gages on girders C & D over Pier 7 were installed after the girders and form work were in place. Theoretical values from TYLI and the Sap IV program were corrected to account for girder prestress and girder and formwork dead load. Good correlation exists between the three methods with the Sap IV values for the bottom flange more in tension than measured on both C & D girder locations (Figs 20 & 21).

The high compressive stresses in top flanges of girders C & D over pier 5 (Fig. 18 & 19) might be explained by analyses of strain data obtained during post-tensioning. Analysis of strain data recorded from girder C after post-tensioning but before girder erection gave the following strain values: top flange strain -866 $\mu\epsilon$, middle -189 $\mu\epsilon$, and

+61.5 $\mu\epsilon$ at the bottom flange (ave. value.) The middle strain value was recorded from the horizontal element of a strain rosette located 40.75 inches from the top flange. Clearly the strain distribution is not linear with depth (Fig. 26). If the middle strain value is neglected and a linear strain distribution is assumed, the total horizontal force calculated from this linear distribution gave 786 kips compression as compared to the total horizontal prestressing force of 621 kips. However, if a non-linear stress distribution (parabolic) is assumed the resulting calculated horizontal force is 666 kips compression.

Four factors were hypothesized as an explanation of the non-linear strain distribution. (Non-linear strain distribution also occurs in webs of steel plate girders designed in accordance with AASHTO design specifications.)

- 1) girder length to depth ratio, $62/6.96 = 8.9$
- 2) possible web warping during the stressing sequence
- 3) depth of the web compared to web thickness (Figures 8, 11).
- 4) Location of stiffners and their effect (Figures 8, 11).

Assuming the non-linear strain relationship holds, the stress value calculated by both analytical methods would give post-tensioning compressive stress values on the top flange lower than the field values and higher tensile stress values on the bottom flange, as previously noted. This condition would hold for the entire time-history as Figures 18 and 19 indicate.

Deck Gages

The working deck gages' computed stress values are listed in Table 3. The longitudinal deck gages are located over piers 5 and 7, and in span

5-6. The lateral gages are located at pier 5 and in span 5-6. The lateral gage in span 5-6 shows a compressive force of 2000 psi at that location which is the design value. The lateral gage over pier 5 shows a compressive force of 3000 psi which is higher than design values, but it is probable that the gage and the bar it is attached to are experiencing local effects due to the non-homogeneous nature of the concrete deck. The high number of tendons, their plastic conduits, and temperature steel complicate gage placement and gage readings. The two working lateral gages indicate that the concrete is close to design values.

The longitudinal gages in span 5-6 unfortunately did not give reliable measurements during the construction period. Their readings reverse between tension and compression indicating a non-functional gage. Conversely, the longitudinal gages over pier 5 all indicate compressive values at the tendon level of 1000 to 2300 psi. The longitudinal gages over pier 7 also read compression. These values range between 2000 psi and 3000 psi at the tendon level. The remaining functional deck gages all indicate that the concrete deck is in compression. Because at the placement method used to install deck gages, all deck strain measurements were subjected to considerable variability. Any conclusions drawn from these measurements would be highly suspect.

The investigators will only report the measurements as part of the field study.

Live Load Test

Figures 28 - 46 depict influence lines for the live load test conducted in July 1985. The plotted points show the difference from an average of "no load" readings taken on three different dates. The "no load" readings varied little, and any questionable gages were omitted.

The dashed lines represent computer generated values from Sap IV for the test truck.

All of the top flange readings (Figs. 28, 30, 32, 34, 35, 37) show little variation from the "no load" condition. It is probable, along with the added $1\frac{1}{2}$ " deck overlay, the actual modular ratio is less than $n = 7$ (i.e. the concrete is stiffer). A stiffer deck would exhibit smaller strains than predicted, and it would raise the neutral axis reducing the gage's readings. In contrast, the bottom flanges of the girders C & D exhibit stresses closer to predicted (Figs. 29, 31, 33, 36 38 & 40). Figure 28 for girder C at pier 5 is almost a one to one plot of predicted and actual values. At span 5 - 6 the plots correlate well (Figs. 30, 31) with the actual peaks well below predicted values.

Two things are important to note on Figs. 30, 31:

First; the D line girder reacts to the loads more than the C line girder. The D line is the outside (East) girder. The load of the test truck and the northbound lane of traffic falls completely on girder D. The loads on girder C are shared with D & B. (Figs. 27)

Second; the reaction of the bridge at the secondary peaks is close to or exceeds that predicted. (Figs. 29, 31, 33, 36, 38).

The predicted values used for comparison were calculated from computer generated stresses using TYLI's design geometric and material properties. Load factors were omitted in the calculations. It is our contention that the modulus values used for the prestressed concrete design contribute to the differences with the bridge field readings.

Transverse deck strain was measured at Pier 5 (Fig. 41) and at span 5 - 6 (Figs. 42, 43) from the working deck gages over girder C. A transverse moment was determined from measured values when the truck was over the C girder in mid-span 5 - 6. (Figs. 42, 43) Fig. 42 represents the change in stress from "no load" condition. The calculated moment from this couple is one fourth that used in design without load factors.

Figures 44 - 46 show longitudinal influence plots for the deck at Pier 7. These figures are noteworthy because they show the increased effect of the load when it is in the outside lane. The outside loading (over Girder D) produces as much stress on the inside (Girder C) as does loading over Girder D.

SUMMARY AND RECOMMENDATION

1. Bridge structural response (with the exception of some of the deck readings) as measured in this investigation are within design specifications after load factors are removed.
2. The top flange girders stresses calculated from field strain measurements were consistently higher in compression than design and computer calculated stresses, while the stresses on the bottom flange were lower in tension than design and computer calculated values. This pattern may be attributed to the following:
 - a. Effective width of deck used in design calculations.
 - b. The added $1\frac{1}{2}$ " overlay.
 - c. Higher actual concrete modulus values than used in the design procedure.
 - d. Effects of parapet, and other stiffening factors not included in design calculations.
 - e. Effects of the post-tensioning non-linearities.
3. The depth of web to thickness ratio was well within design specifications for plate girders at the design loads, however measurements indicated the top girder compression flange carried more stress after post-tensioning than predicted by beam theory. High stressing levels on the relatively slender plate girder (depth of web/thickness of web = 170) are assumed to cause the non-linear strain distribution as measured in the girders over pier 5.
4. A more complete strain measurement over the depth of the beam during the post-tensioning sequence should be made to determine the extent of strain non-linearities.
5. Live load tests showed bridge longitudinal stresses

consistently lower than predicted at the peak values, but the secondary peak values were close to design values.

6. All deck strain measurements exhibited considerable variability. Conclusions drawn from these values would be highly suspect. Only in the relative comparisons between the "no load" and live load test did the measurement show consistent behavior.

Table 1

Pretensioning of Girders C & D, Pier 5, 21 September 1983.

STRESSING ORDER (GIRDERS C & D CONNECTED BY DIAPHRAGMS)	MONITORED TENDON PRESTRESSING FORCE IN KIPS (1)		
	TENDON A	TENDON B	TENDON C
1. TENDON A, GIRDER D			
a. Prior to release of jacking head	216		
b. After release of jacking head	199		
2. TENDON A, GIRDER C			
a. Prior to release of jacking head	229		199
b. After release of jacking head	216		199
3. TENDON B, GIRDER C			
a. Prior to release of jacking head	210	218	199
b. After release of jacking head	210	205	199
4. TENDON C, GIRDER C			
a. Prior to release of jacking head	200	199	236
b. After release of jacking head	200	199	222
5. TENDON B, GIRDER D			
a. Prior to release of jacking head	200	199	222
b. After release of jacking head	200	199	193
6. TENDON C, GIRDER D			
a. Prior to release of jacking head	200	199	186
b. After release of jacking head	200	199	186
CALCULATED VALUES	201	198	222
NOTES: Tendon prestressing force measured with load rings.	184	205	205
Tendon B denotes outside tendon on west side of girder.	230		
Tendon C denotes outside tendon on east side of girder.	220		

Table 2
Tabulated Time History of Stresses (ksi)

Gage		1983		1984											
No.	Location	9-14	11-12	11-20	1-29	2-20	3-18	3-24	4-1	4-12	4-28	5-24	9-21	11-2	
5	P8, GC, TF	-	36.00	30.96	31.62	30.68	30.08	30.48	30.78	30.59	29.53	28.23	26.21	25.71	
6	P8, GC, TF	-	32.61	29.01	29.84	28.55	28.43	28.83	29.21	29.97	27.77	26.42	24.53	23.85	
8	P8, GC, BF	-	-13.15	-14.32	-12.90	-13.35	-13.19	-12.75	-12.90	-12.93	-13.39	-13.73	-15.19	-15.74	
9	P8, GC, BF	-	-16.78	-17.38	-15.66	-16.66	-16.26	-15.55	-15.71	-15.60	-16.52	-17.11	-18.61	-19.56	
13	P8, GD, TF	5.30	33.09	30.17	30.98	30.02	29.37	29.43	29.97	29.61	28.77	28.88	27.67	27.12	
14	P8, GD, TF	3.45	29.44	25.85	26.51	25.38	24.99	25.25	25.43	25.12	24.14	24.33	21.94	21.24	
15	P8, GD, BF	-1.24	-12.37	-14.08	-13.20	-14.16	-14.40	-14.51	-14.22	-14.31	-16.50	-15.37	-16.30	-16.99	
16	P8, GD, BF	-1.78	-14.03	-14.53	-13.02	-14.25	-13.72	-14.09	-14.06	-13.73	-16.39	-16.38	-17.32	-18.60	
25	S5-6, GC, TF	-	2.86	2.13	-3.39	-4.7	-1.16	-1.86	-22.79	-18.79	-18.99	-19.51	18.84	-19.01	
26	S5-6, GC, TF	-	1.70	.81	-1.81	-1.74	-2.37	-3.30	-22.77	-19.25	-19.43	-19.87	-19.44	-19.52	
27	S5-6, GC, BF	-	1.43	-	.78	2.32	2.14	2.88	13.88	11.77	10.19	11.34	10.02	11.72	
28	S5-6, GC, BF	-	-.36	-	.22	-.23	.29	.87	12.32	9.63	8.07	8.95	7.86	7.70	
36	S5-6, GD, TF	-	7.55	6.67	3.74	3.69	2.83	2.24	16.95	-15.38	-14.45	-14.50	-13.41	-13.37	
37	S5-6, GD, TF	-	6.69	5.75	3.09	3.19	1.28	-.61	-18.19	-16.84	-16.20	-16.76	-16.40	-15.96	
38	S5-6, GD, BF	-	-.54	-1.02	-.12	-.61	.20	.63	11.54	9.10	7.03	8.95	7.65	8.00	
39	S5-6, GD, BF	-	.57	.41	-.22	1.14	1.26	2.35	12.18	8.13	7.99	10.21	8.37	10.45	
59	P5, GC, TF	24.08	-22.24	-24.51	-22.68	-21.91	-21.58	-21.45	-12.25	9.19	8.38	2.03	-1.81	-2.39	
60	P5, GC, TF	26.11	-27.50	-28.61	-26.92	-25.77	-25.61	-25.31	-14.21	7.69	6.43	.58	-2.67	-3.33	
64	P5, GC, BF	2.15	1.33	1.24	1.61	-.89	1.04	-.29	-.77	-17.46	-18.67	-16.84	-19.35	-20.11	
65	P5, GC, BF	2.10	1.09	2.98	2.25	1.90	1.92	-1.22	-8.07	-17.64	-18.50	-16.54	-18.29	-18.15	
66	P5, GD, TF	22.45	-23.34	-24.20	-22.81	-22.03	-20.90	-20.74	-11.86	7.42	5.52	-.59	-4.26	-5.14	
67	P5, GD, TF	25.55	-26.01	-26.78	-26.10	-24.68	-23.79	-23.68	-14.01	4.40	2.79	-2.59	-5.56	-6.44	
72	P5, GD, BF	5.07	8.49	20.10	7.89	9.27	21.11	14.12	8.44	-.68	22.44	7.59	-9.00	-13.61	
73	P5, GD, BF	2.73	.98	-.26	.25	-2.20	-2.57	-2.10	-7.80	-17.66	-16.39	-14.82	-17.06	-17.64	
62	P5, GC, HR	-	-4.42	-	-5.96	-5.14	-5.40	-5.15	-5.06	-1.12	-2.19	-3.68	-6.86	-6.62	
62.5	P5, GC, DR	-	2.45	-	-.98	.50	.18	.15	1.88	9.68	9.77	6.92	5.83	5.97	
63	P5, GC, VR	-	14.50	-	18.34	10.88	11.85	11.38	7.34	1.28	.88	2.60	4.60	0.97	
69	P5, GD, HR	-	-26.12	-	-30.81	-27.01	-24.78	-24.41	-14.62	-1.76	-3.01	-6.47	-9.37	-13.10	
69.5	P5, GD, DR	-	-4.05	-	-5.19	-4.27	-4.78	-4.68	-5.30	-3.83	-3.33	-4.15	-5.61	-4.59	
70	P5, GD, VR	-	-.24	-	-1.68	-3.00	-2.60	-2.20	-3.02	-5.89	-5.78	-4.34	-2.25	-3.41	
104	P7, GC, TF	-	-	-4.64	-7.00	-6.71	-7.25	-7.70	-7.09	-7.46	-8.52	-9.18	-11.22	-12.67	
106	P7, GD, TF	-	-	-4.32	-8.00	-5.87	-7.26	-7.35	-7.89	-8.78	-8.89	-9.14	-11.63	-11.54	
107	P7, GD, BF	-	-	-2.81	-4.22	-2.75	-3.30	-4.31	-1.25	-1.76	-2.87	-1.77	-2.25	-2.54	

Notations:

P - Pier

TF - Top Flange

HR - Horizontal Rosette

BF - Bottom Flange

DR - Diagonal Rosette

VR - Vertical Rosette

Table 3

DECK GAGES (STRESS IN KSI)
1984

Notations:	P - Pier	E - East
	GC - Girder C	W - West
	GD - Girder D	L - Longitudinal
	S - Span	T - Transverse

Table 4
 TABULATED TIME HISTORY OF FINITE ELEMENT CALCULATED STRESSES
 DURING CONSTRUCTION

Gage Location	Date					
	10/83	11/83	3/84	4/84	5/84	6/84
P8, GC, TF	21.01	25.14	23.82	23.37	N/C	N/C
P8, GC, BF	-12.30	-14.06	-13.32	-13.07	N/C	N/C
P8, GD, TF	35.00	30.54	+29.41	28.86	N/C	N/C
P8, GD, BF	-16.70	-17.08	-16.45	-16.14	N/C	N/C
P7, GC, TF	13.40	31.86	25.86	27.8	N/C	29.8
P7, GC, BF	11.0	-28.64	-22.64	-23.2	N/C	-19.1
P7, GD, TF	12.50	30.85	21.0	22.7	N/C	28.5
P7, GC, BF	10.01	-28.04	-22.2	23.0	N/C	-17.03
S5-6, GC, TF	2.01	-2.19	N/C	-8.31	-10.03	-9.69
S5-6, GC, BF	-1.70	1.77	N/C	6.72	8.11	7.65
S5-6, GD, TF	6.80	-1.50	N/C	-7.90	-9.72	-9.14
S5-6, GD, BF	-2.50	1.21	N/C	+6.38	7.85	7.40
P5, GC, TF	-9.80	6.08	N/C	28.04	24.6	25.6
P5, GC, BF	2.78	-13.23	N/C	27.0	-23.7	-24.6
P5, GD, TF	-7.50	6.08	N/C	28.04	24.6	25.6
P5, GD, BF	2.50	-13.23	N/C	27.0	-23.7	-24.6

Notations:

P - Pier	TF - Top Flange	HR - Horizontal Rosette
S - Span	BF - Bottom Flange	DR - Diagonal Rosette
GC - Girder C		VR - Vertical Rosette
GD - Girder D		

N/C - No appreciable change

Figure 1

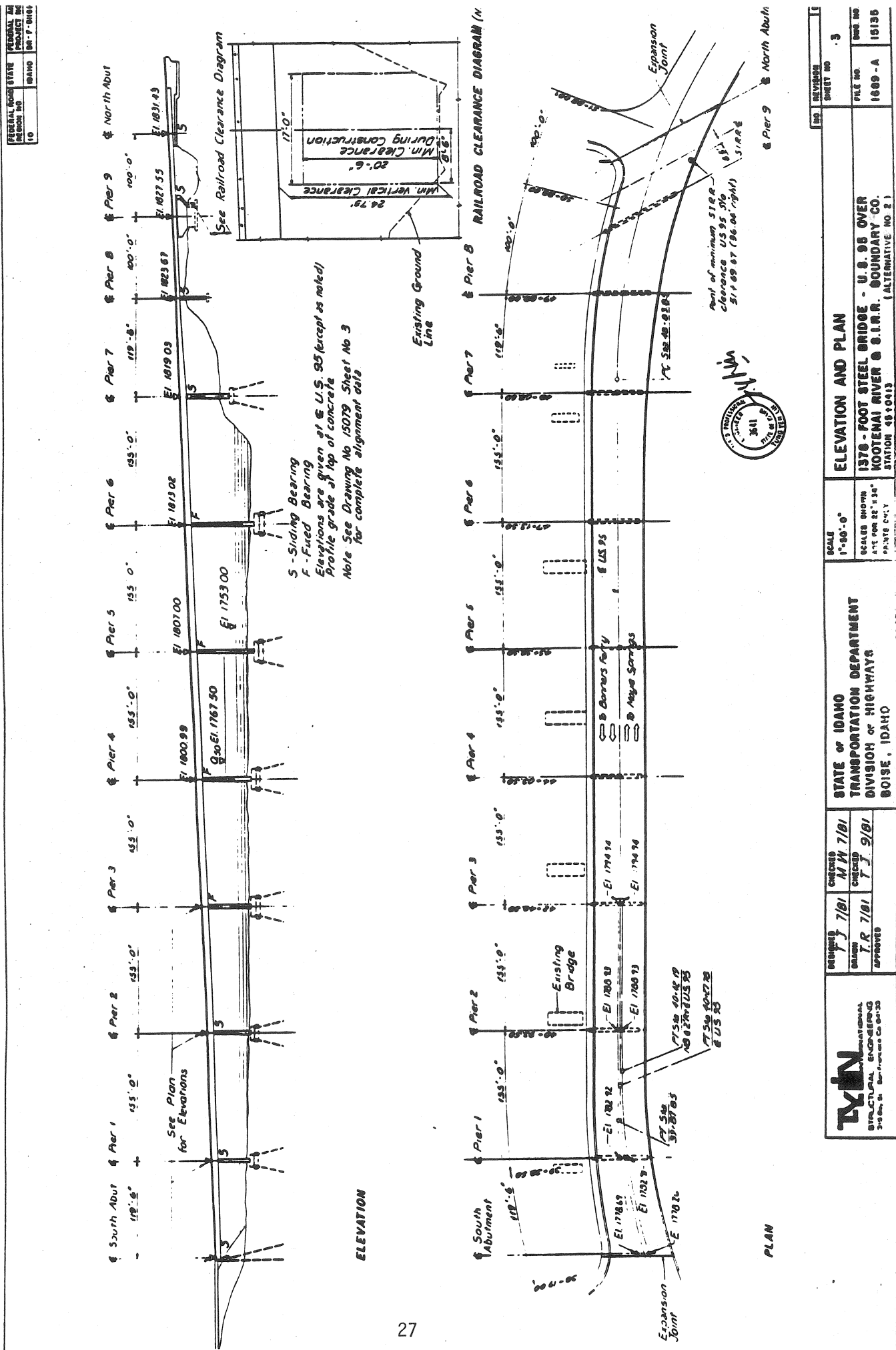


Figure 2

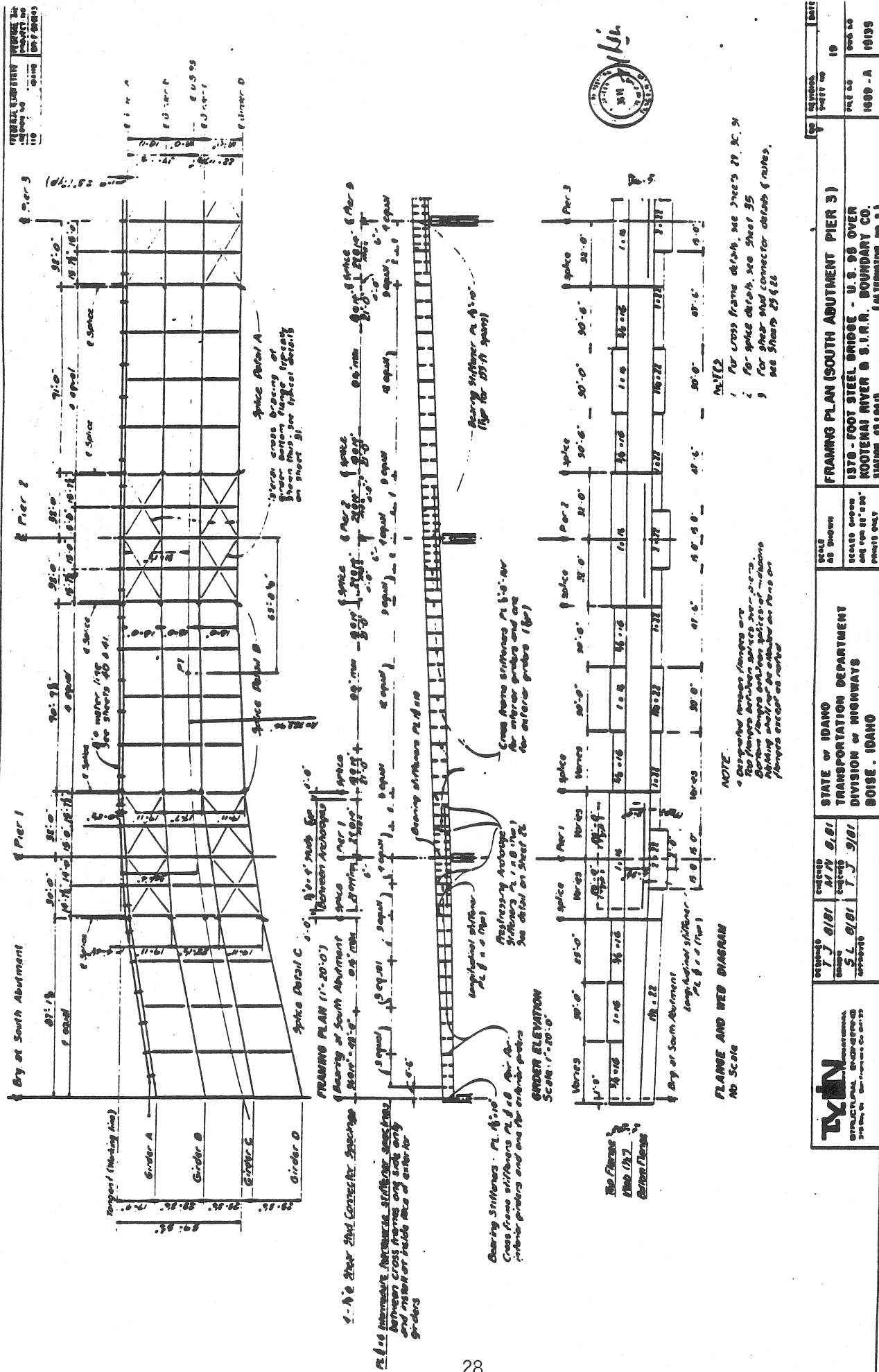


Figure 3

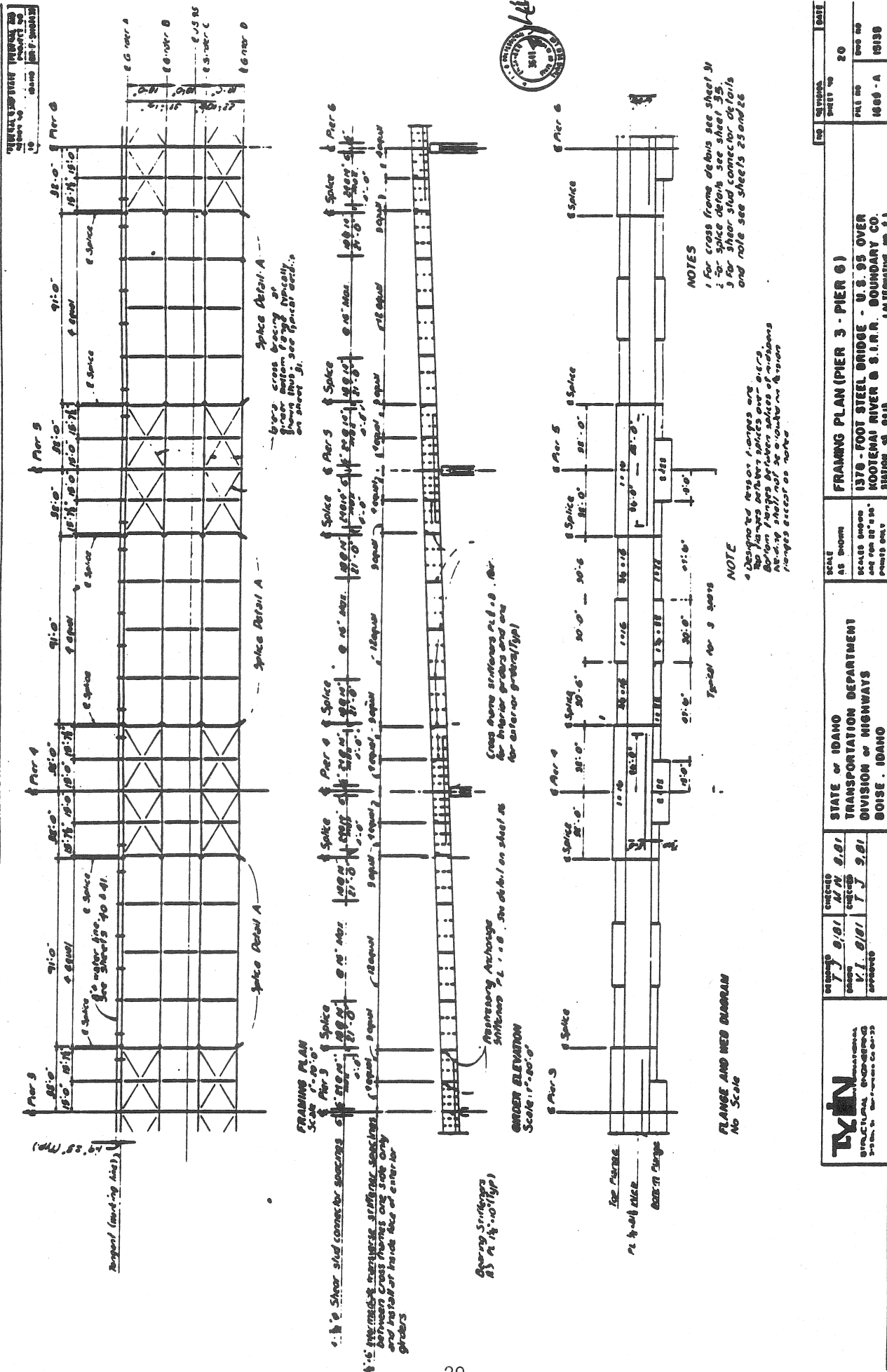


Figure 1

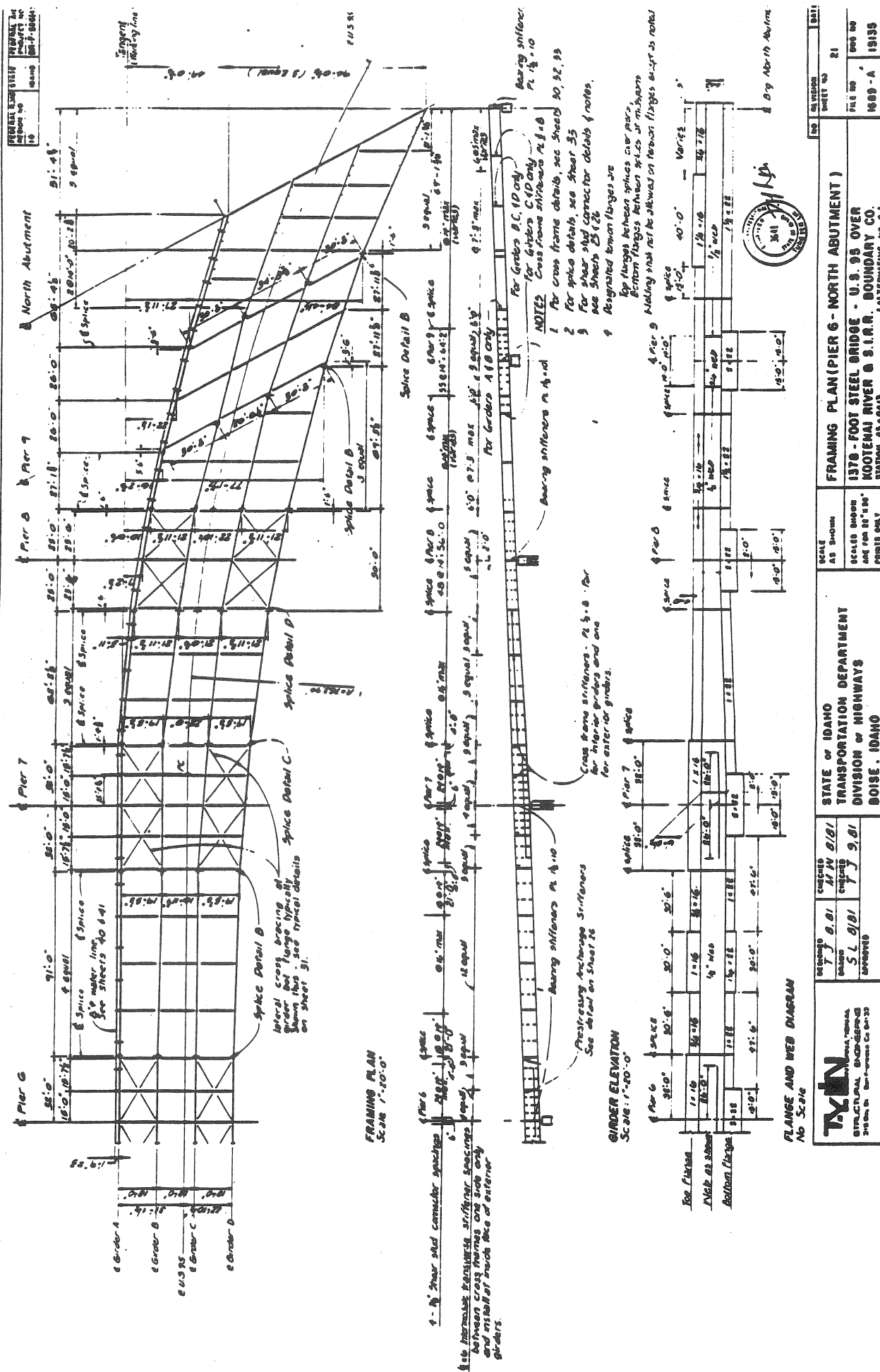
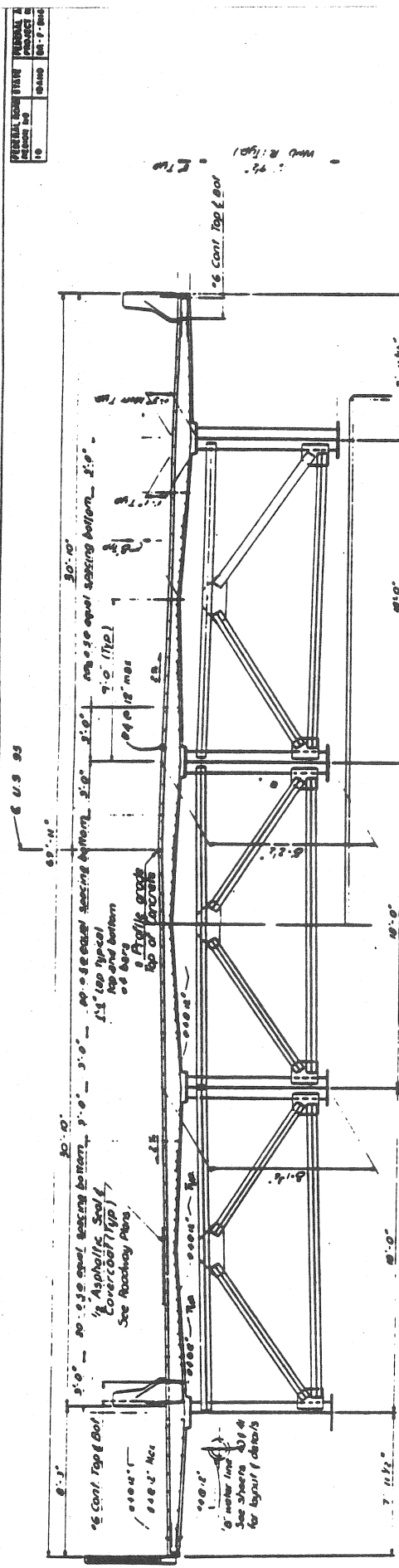
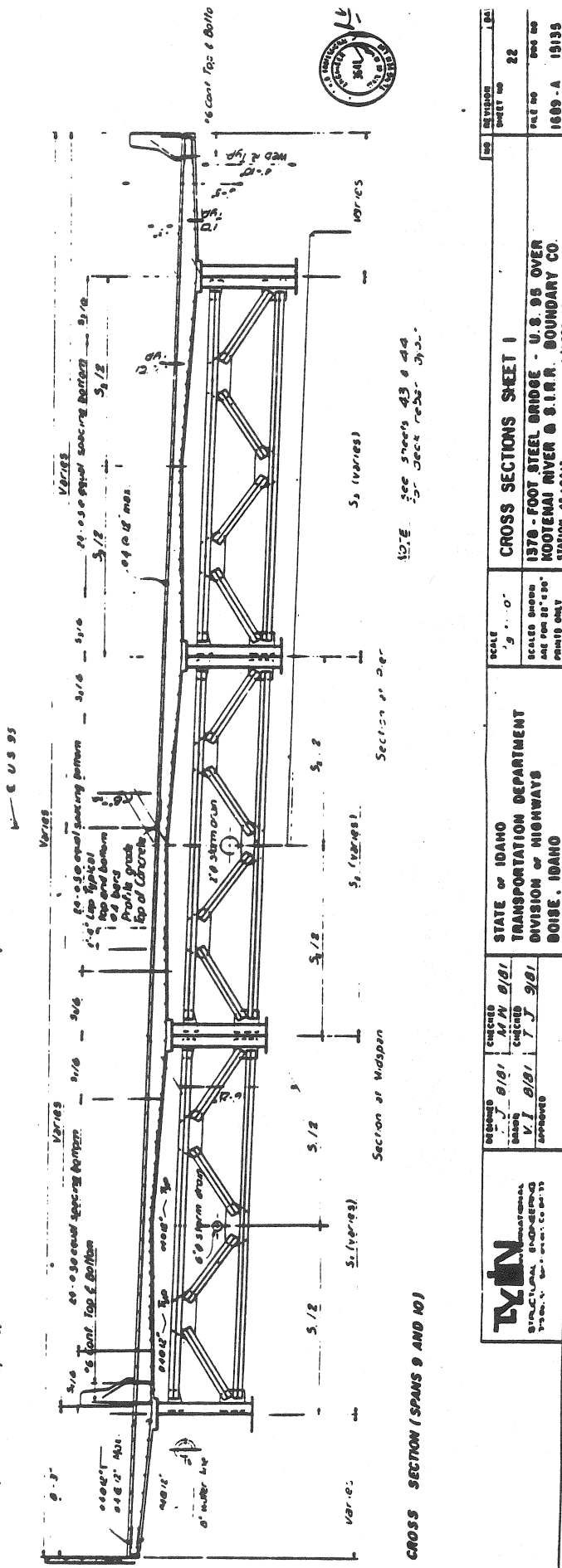


Figure 5



TYPICAL CROSS SECTION (SPANS 3 FEET 0")



CROSS SECTION / SPANS 9 AND 10

Figure 6

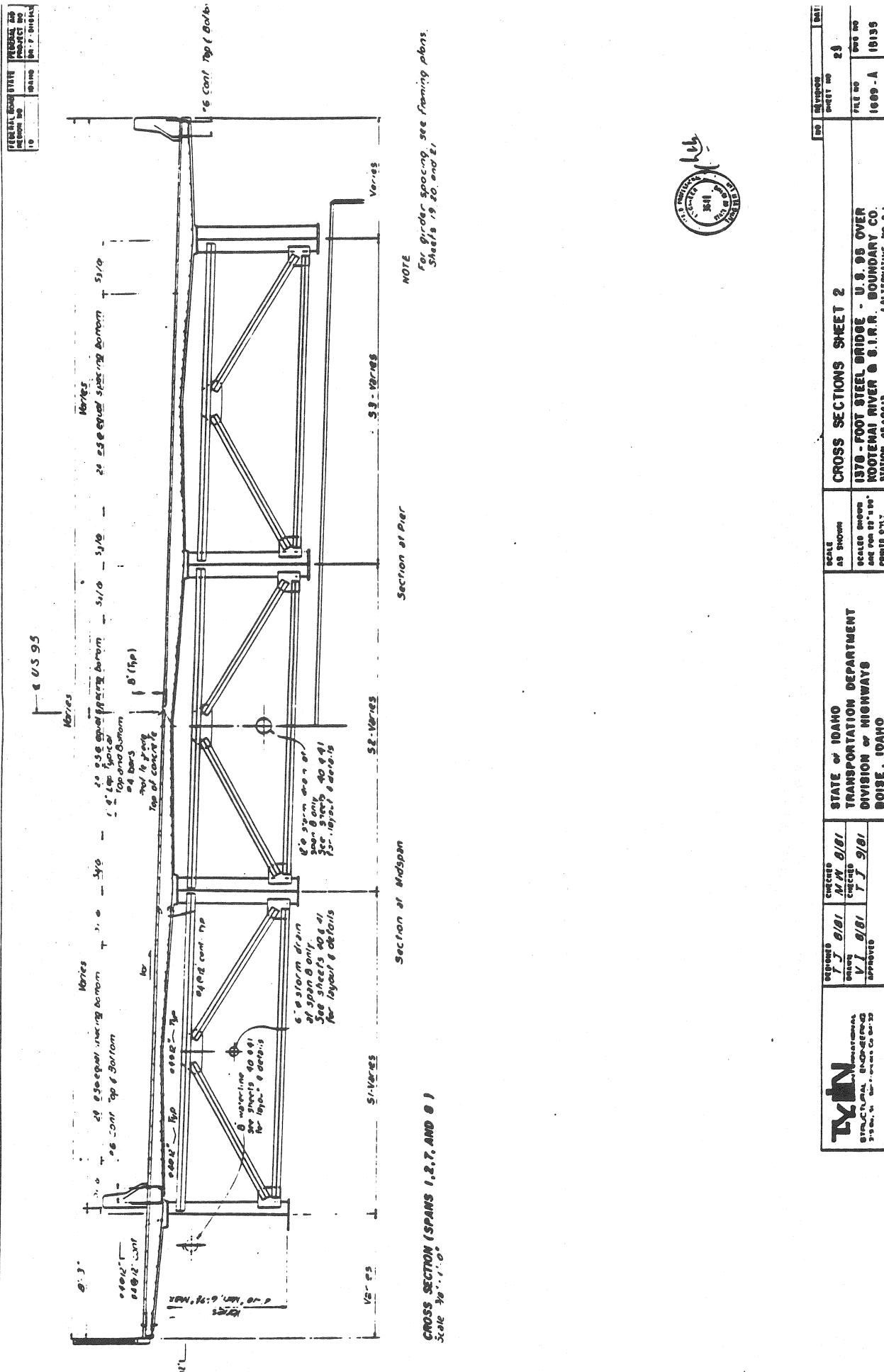


Figure 7

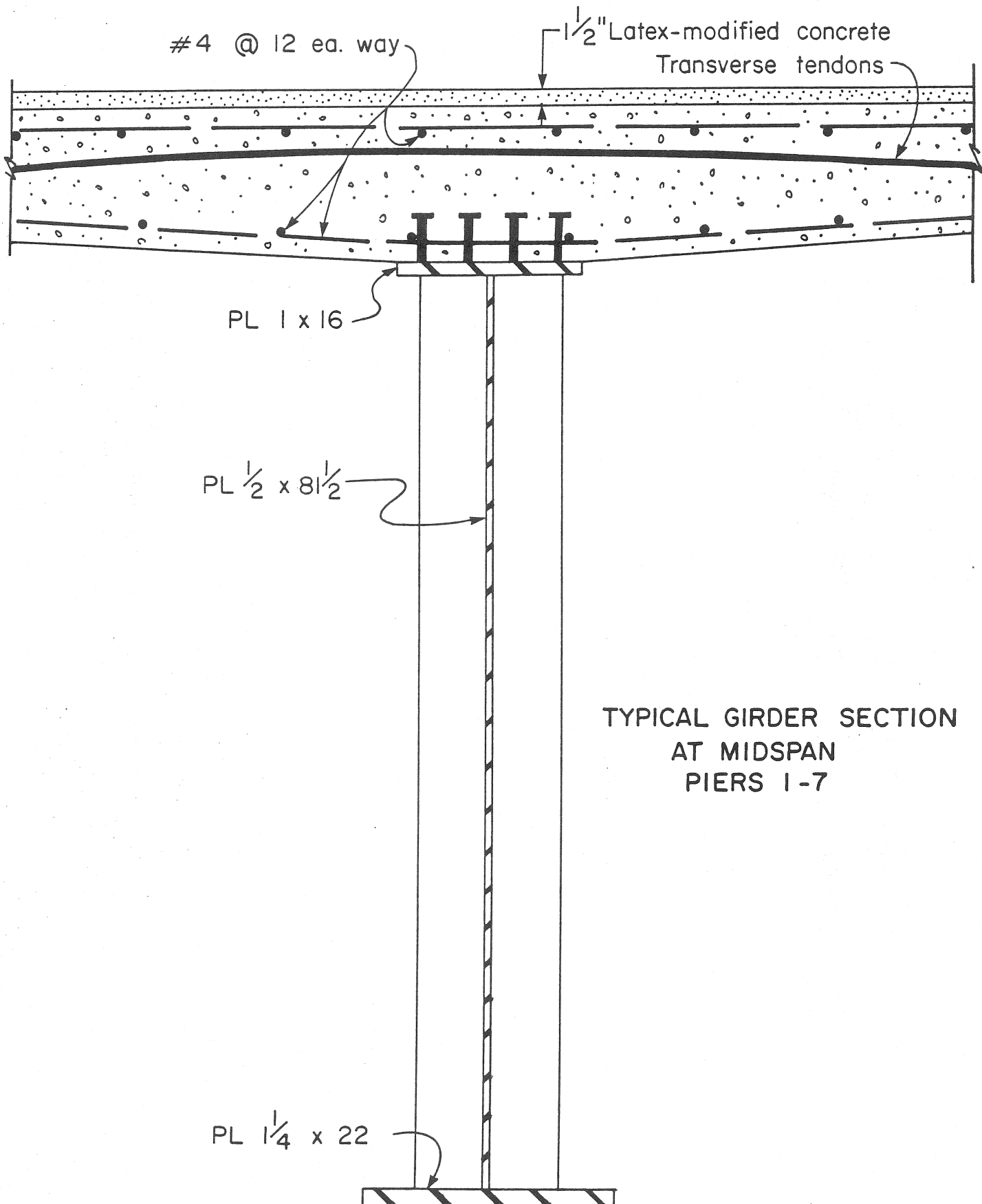


Figure 8

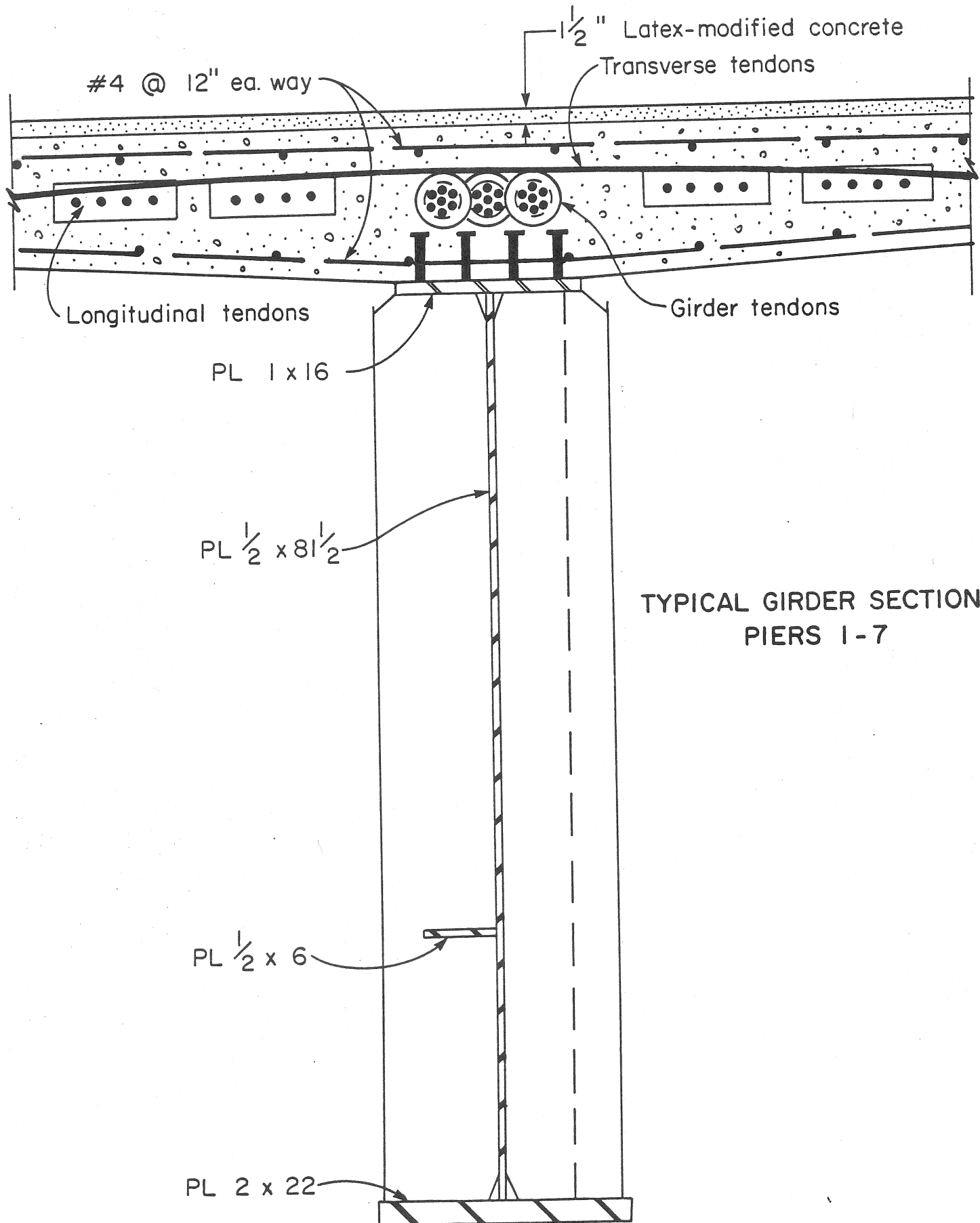


Figure 9

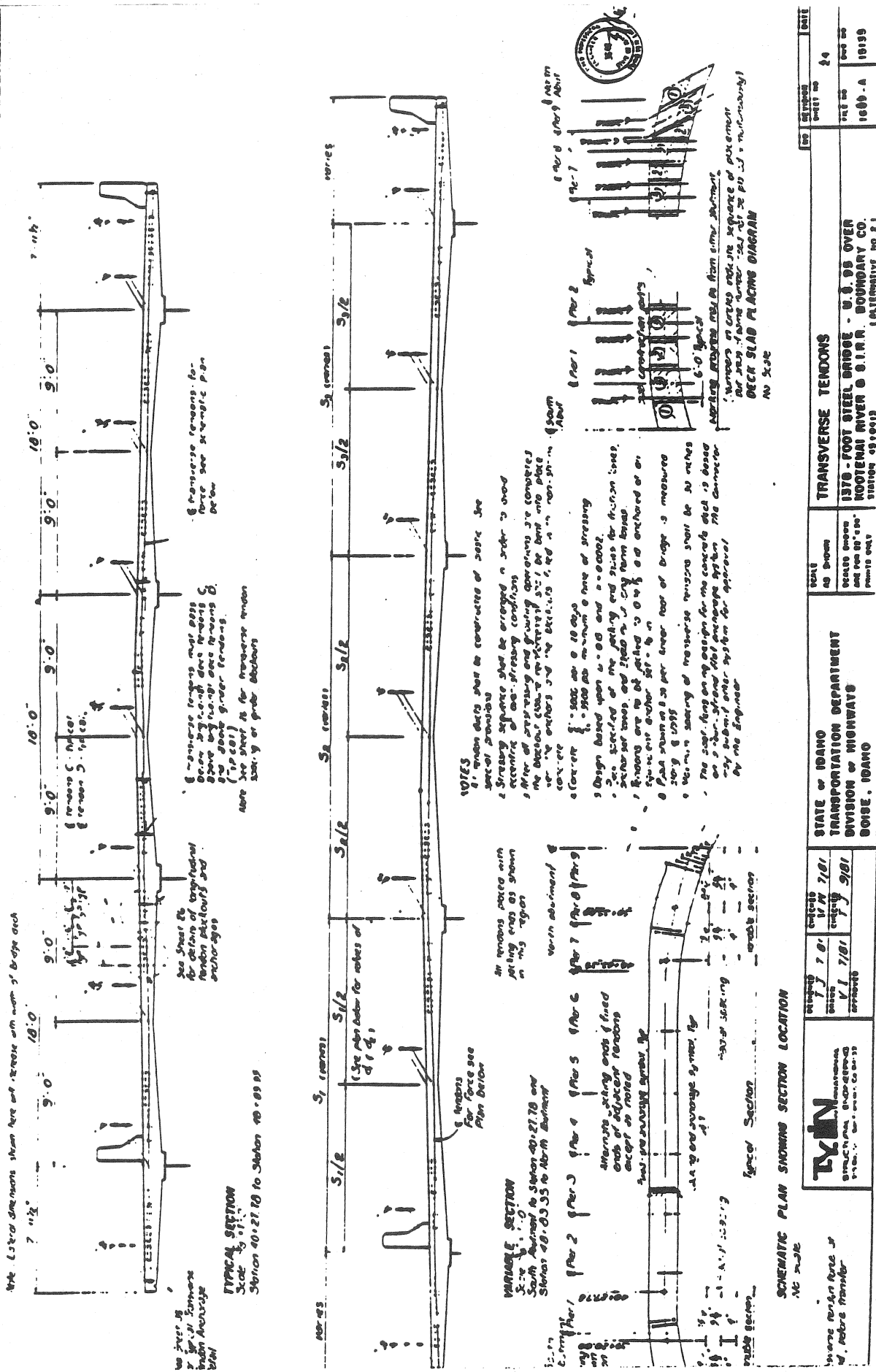


Figure 10

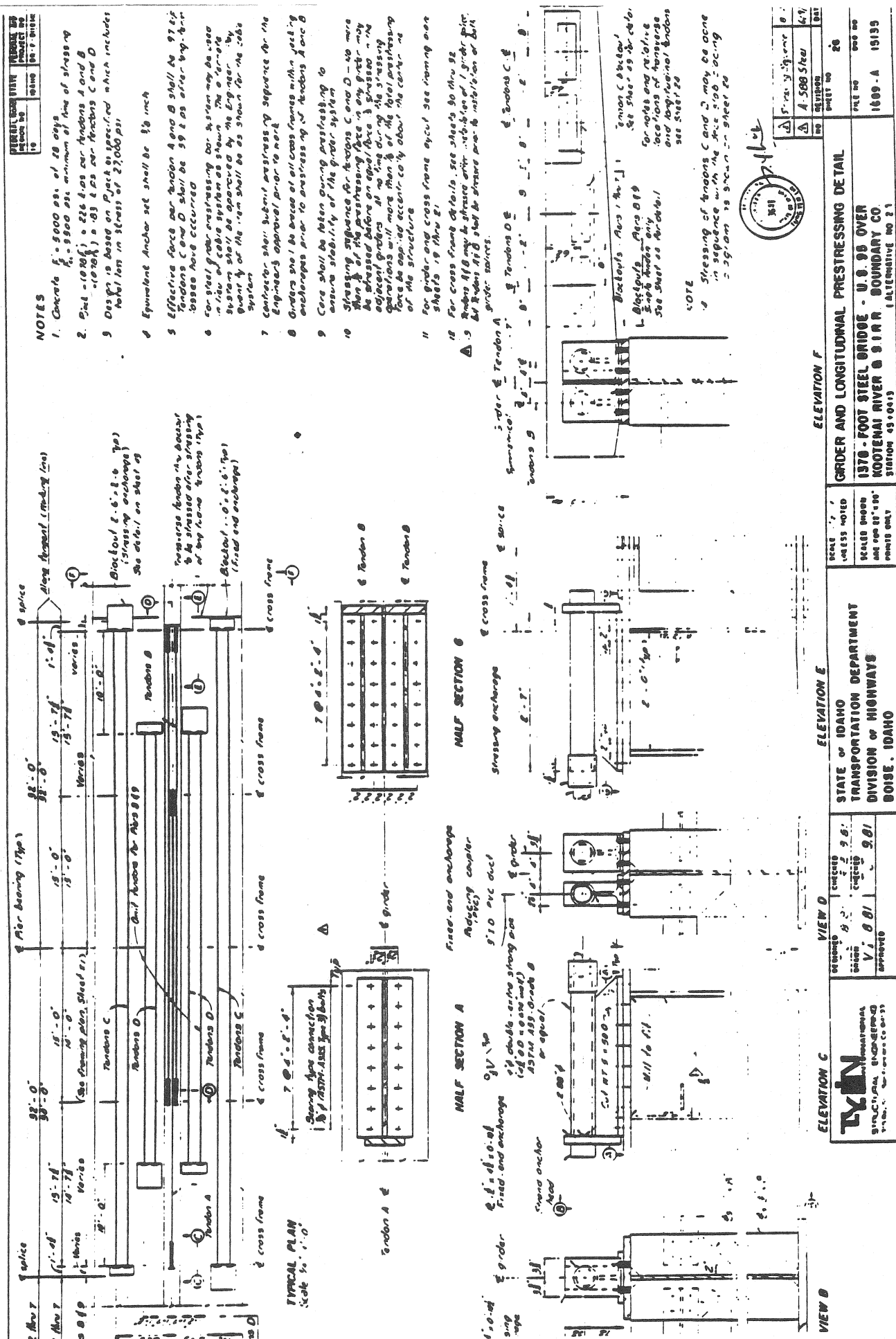


Figure 11

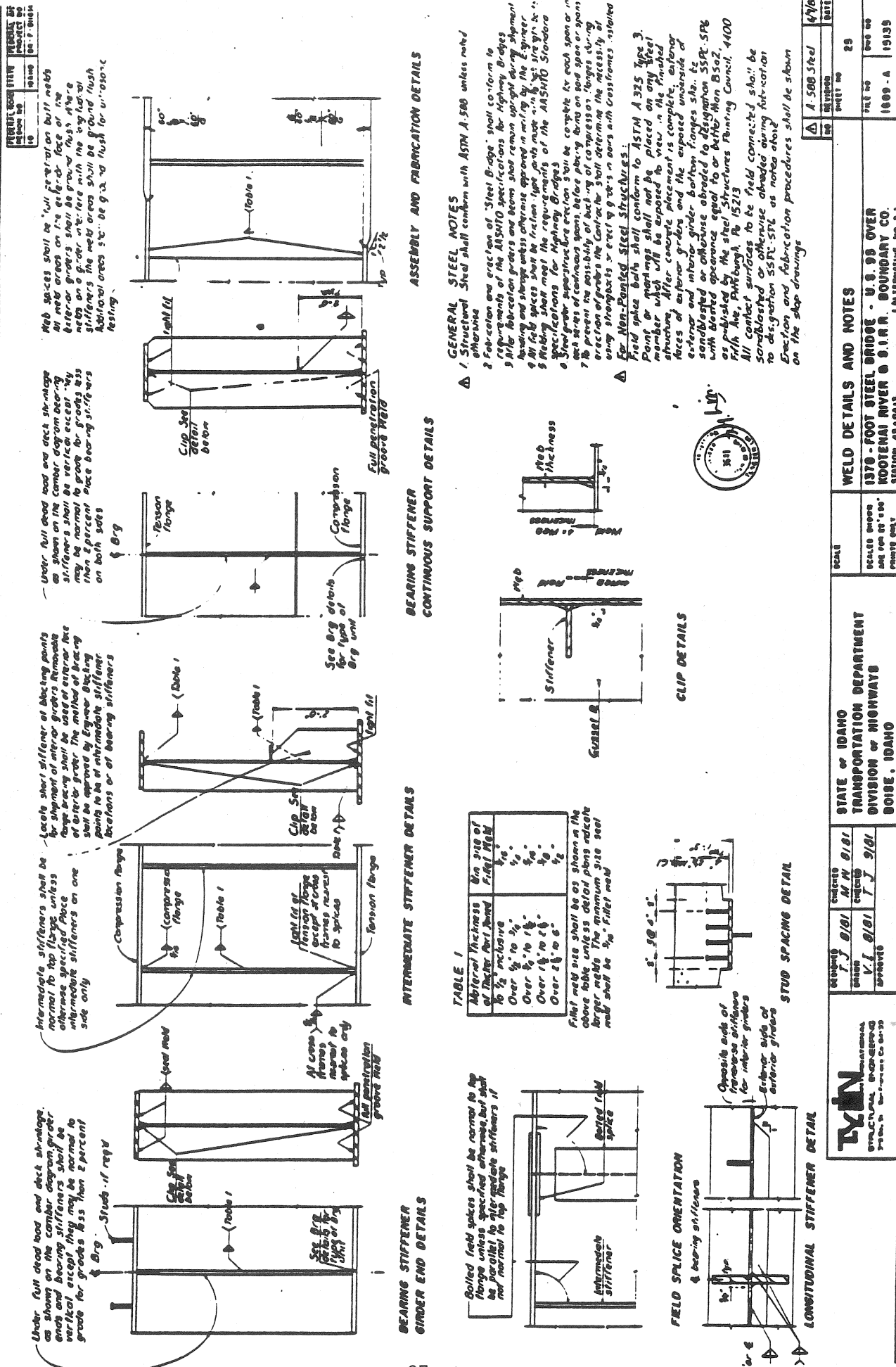


Figure 12

BONNERS FERRY BRIDGE - NORTH END
SUPERSTRUCTURE CONSTRUCTION SEQUENCE

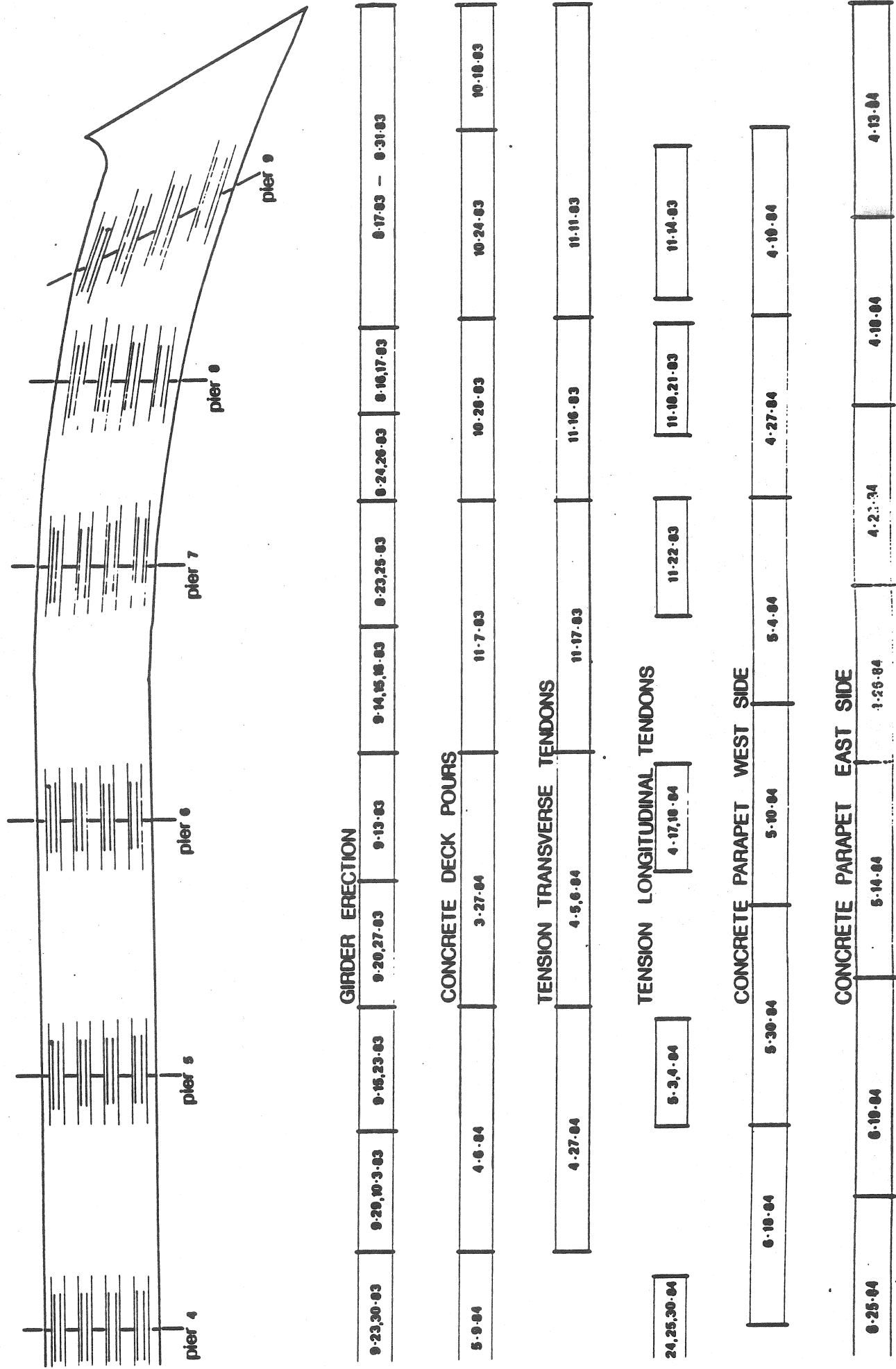
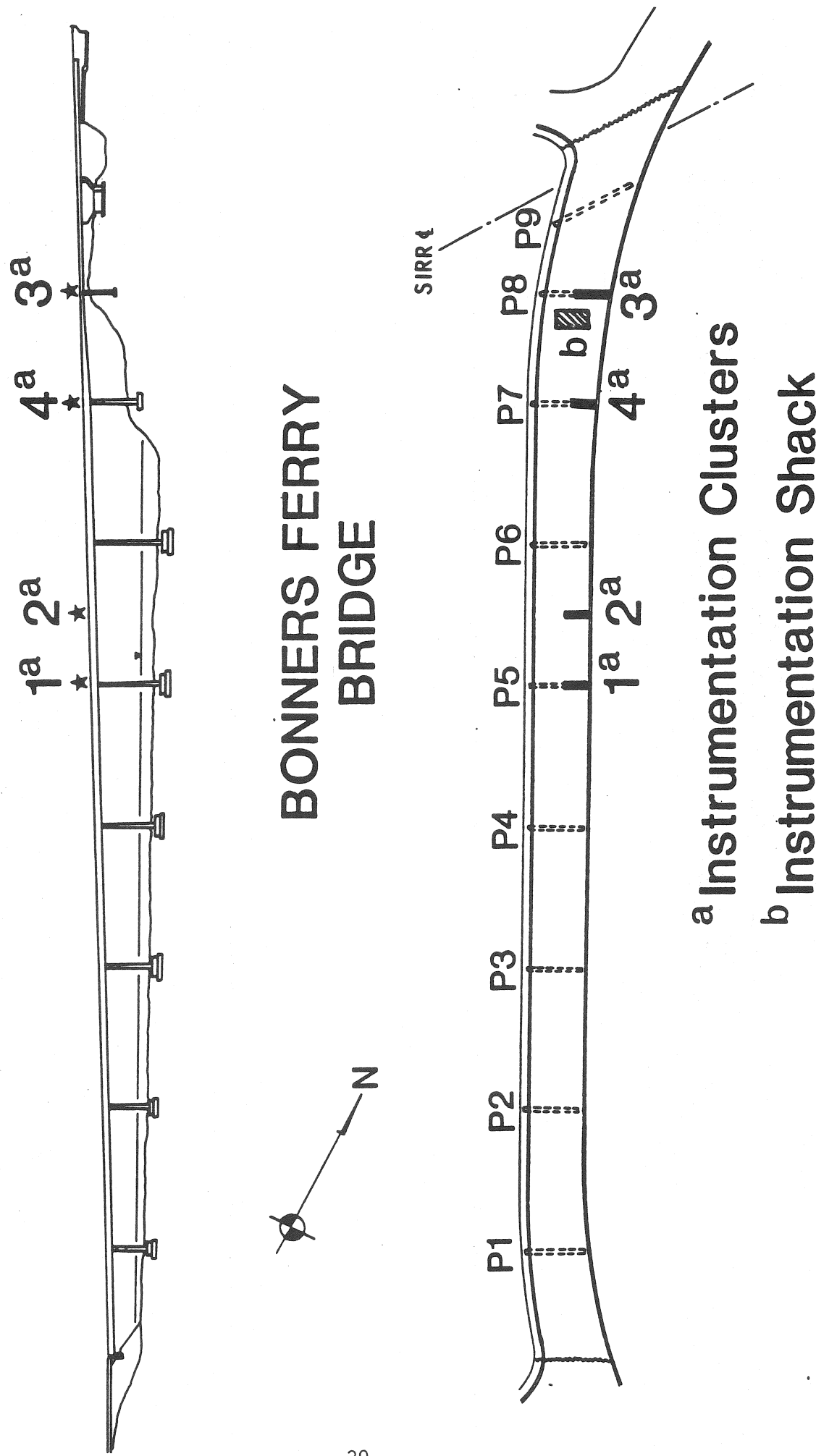


Figure 13



Elevation and Plan of Bonners Ferry Bridge Depicting Instrumentation Locations.

Figure 14

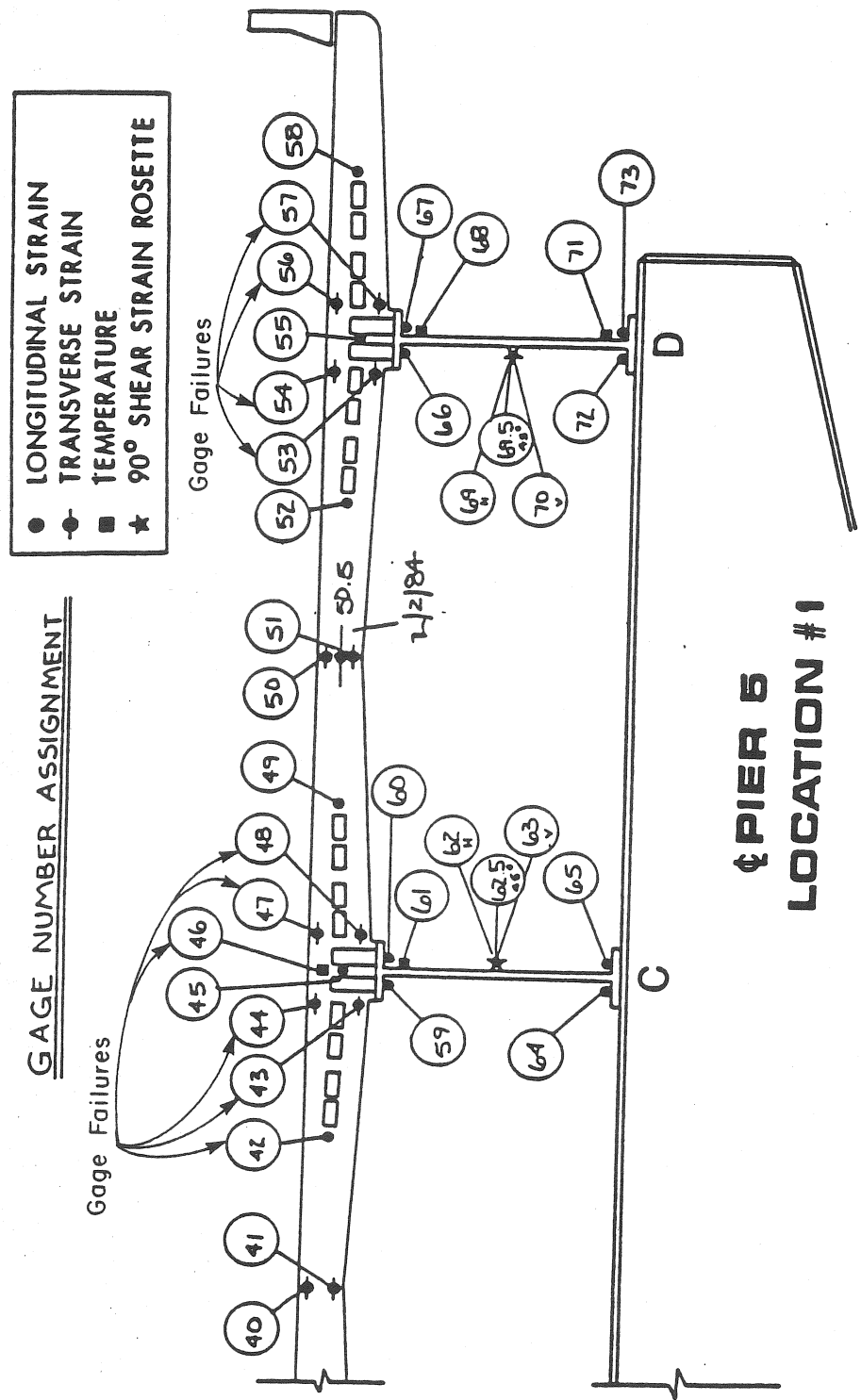


Figure 15

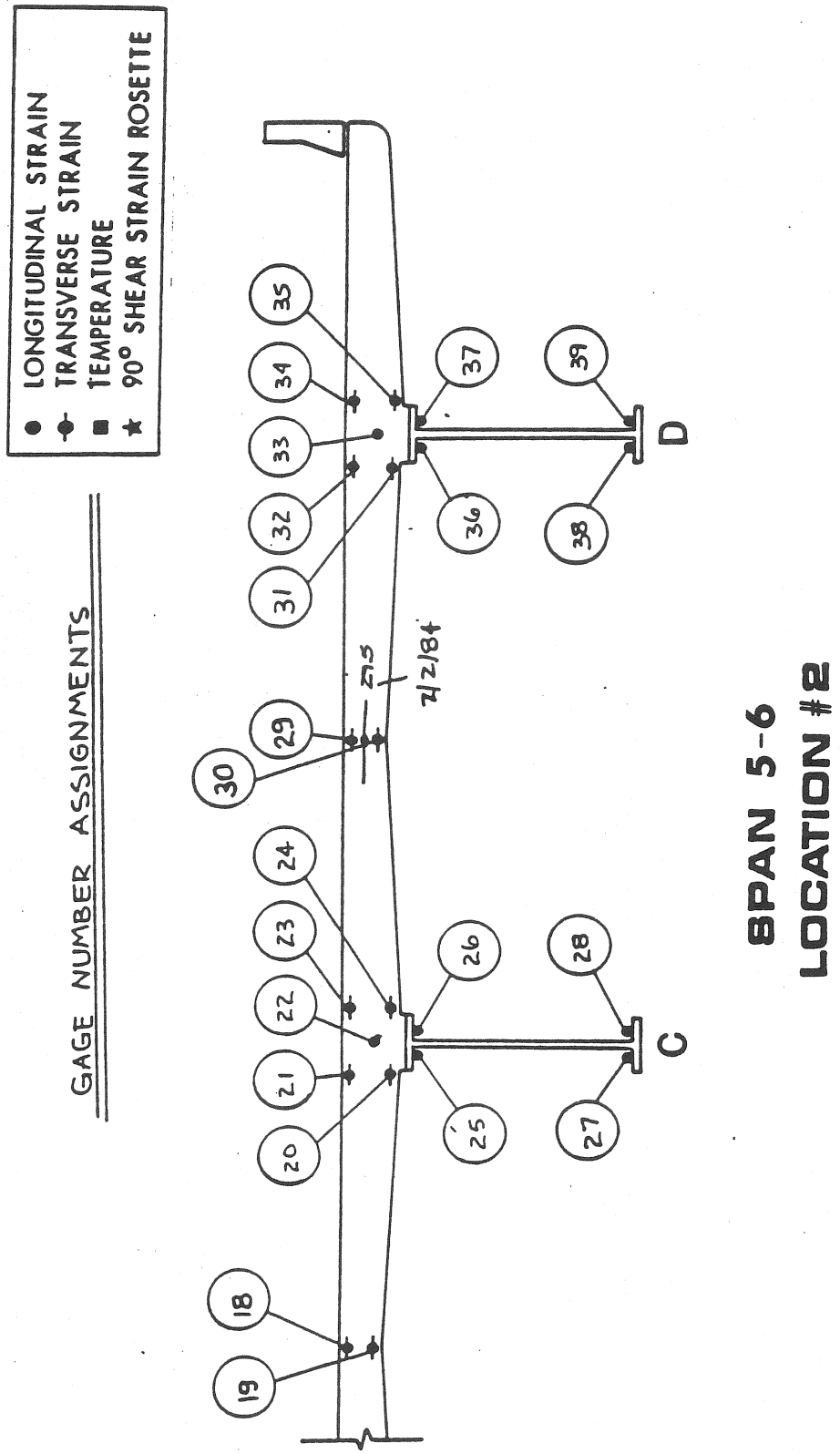


Figure 16

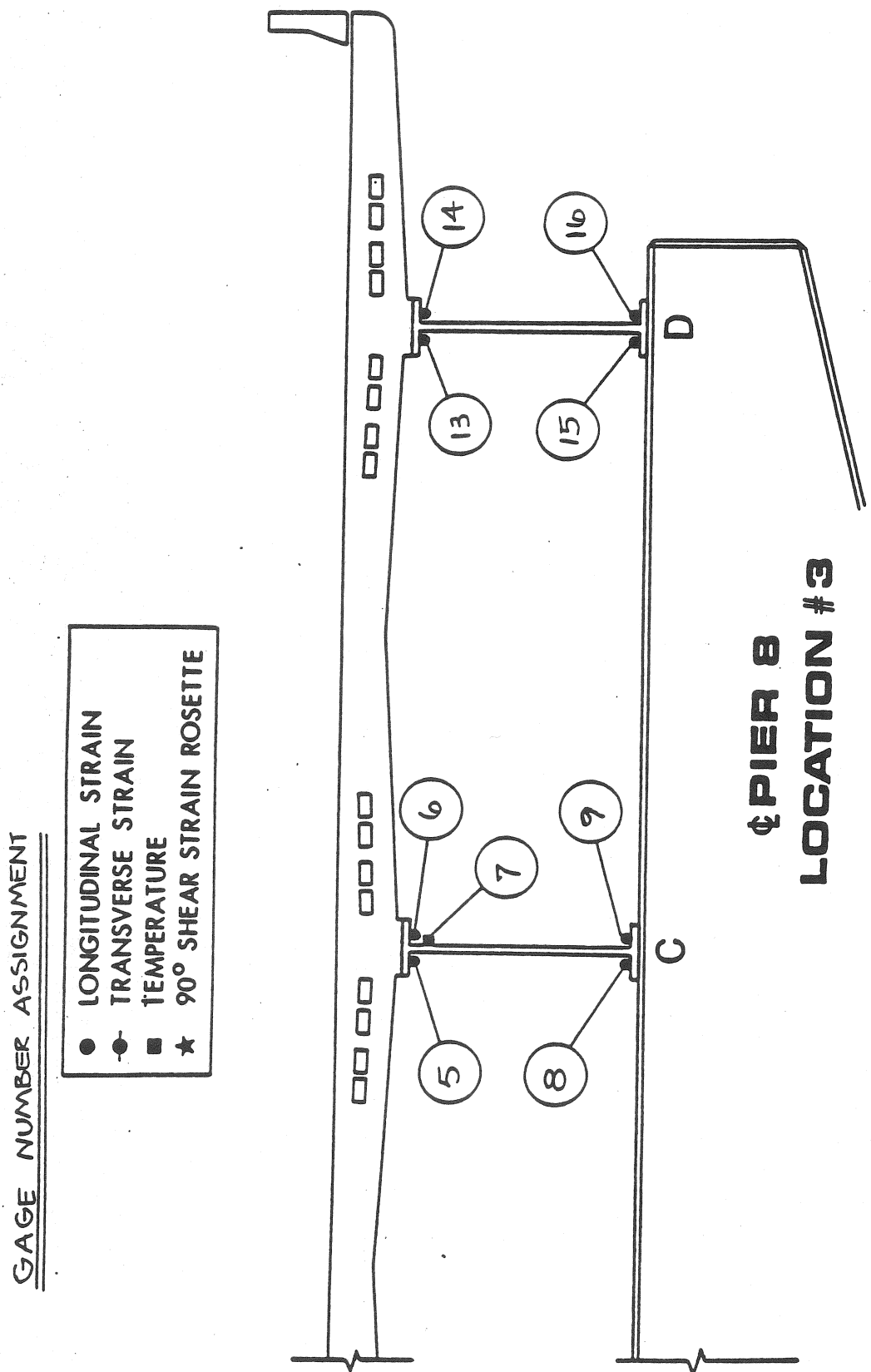
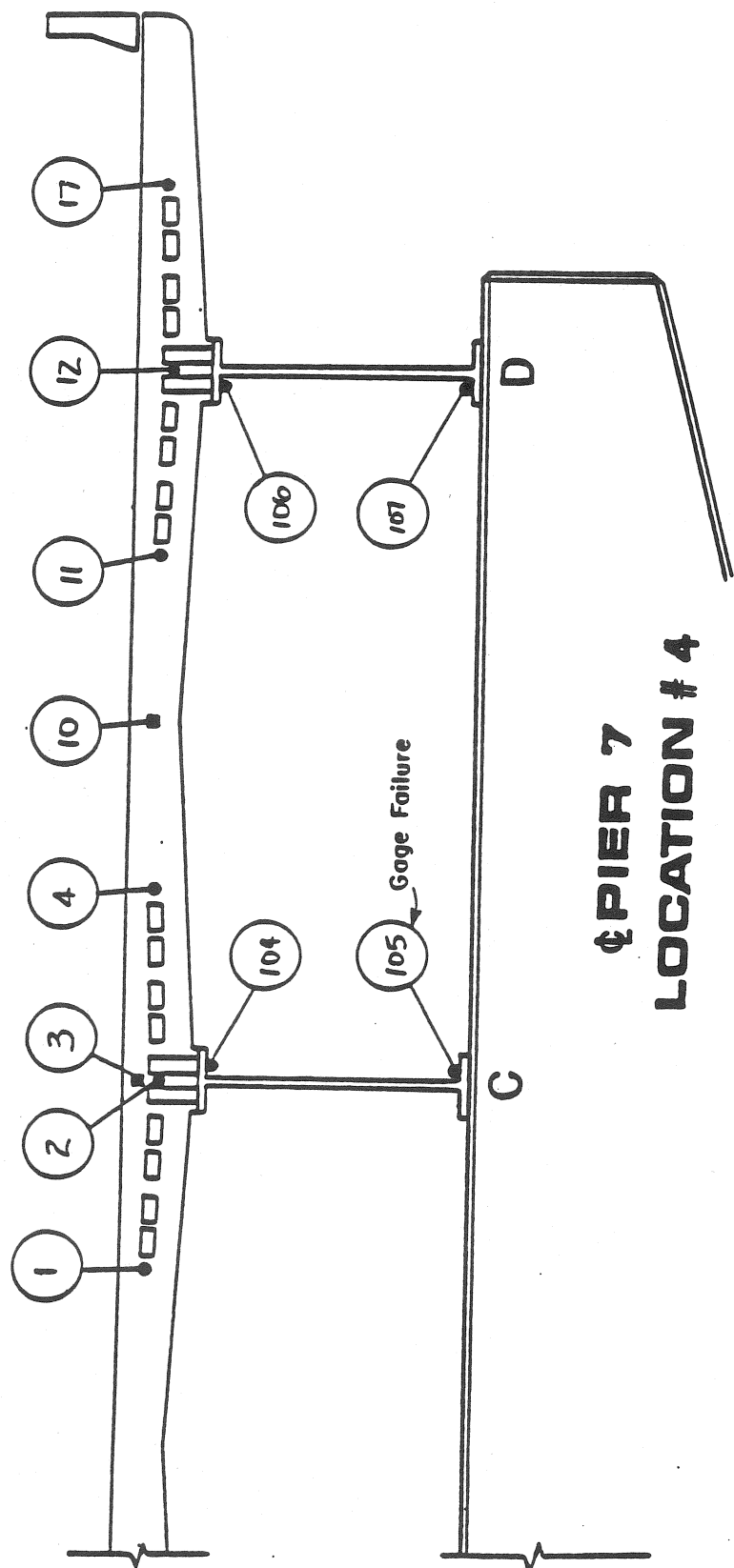


Figure 17

GAGE NUMBER ASSIGNMENT

- LONGITUDINAL STRAIN
- TRANSVERSE STRAIN
- TEMPERATURE
- ★ 90° SHEAR STRAIN ROSETTE



GIRDER GAGE PLACEMENT:
TOP FLANGE

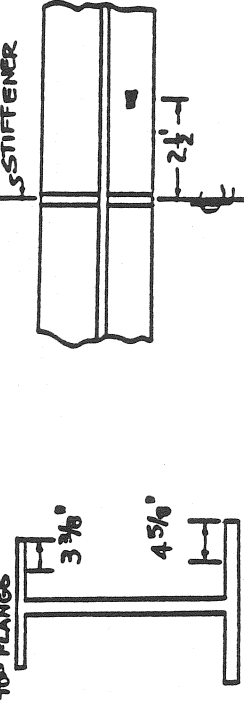


Figure 18

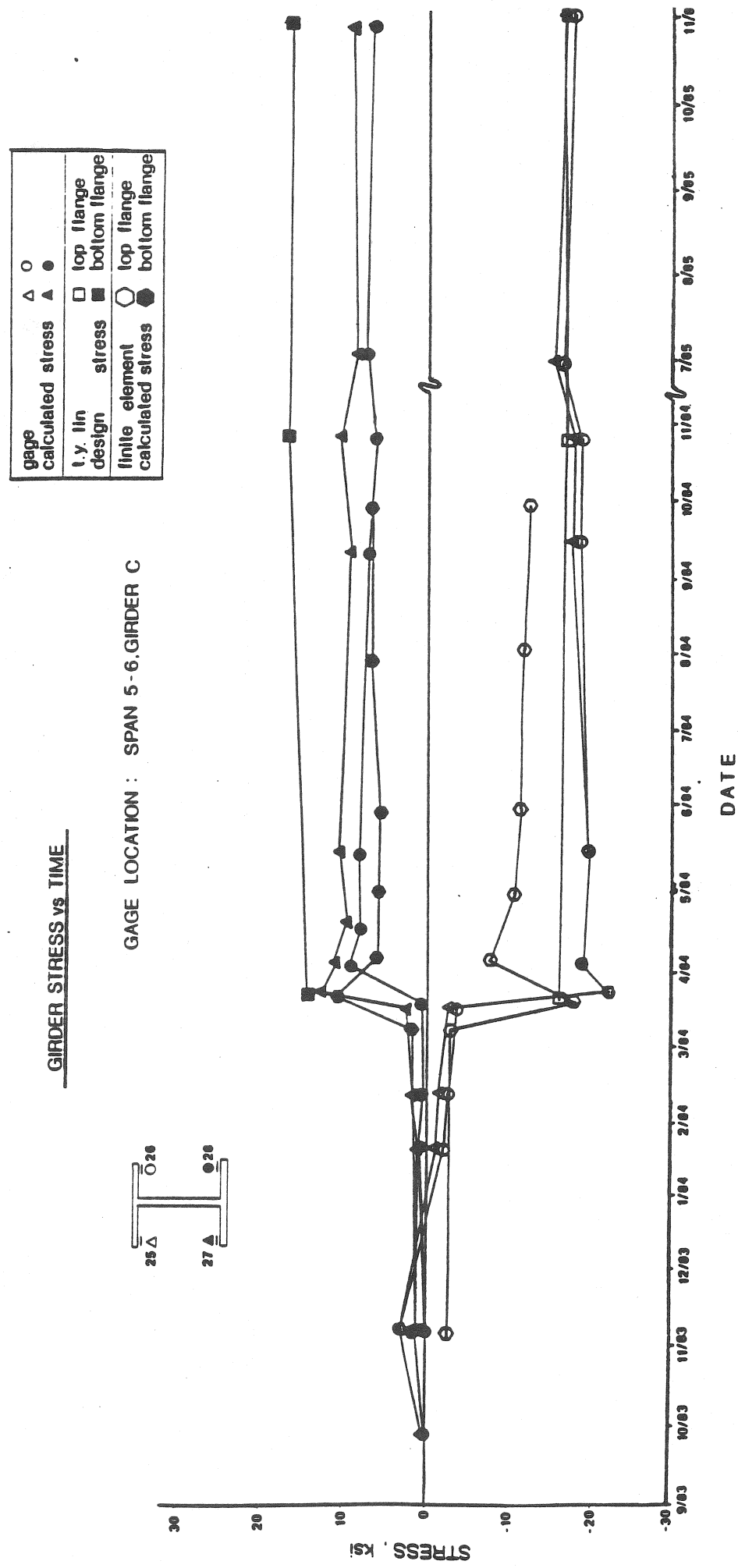


Figure 19

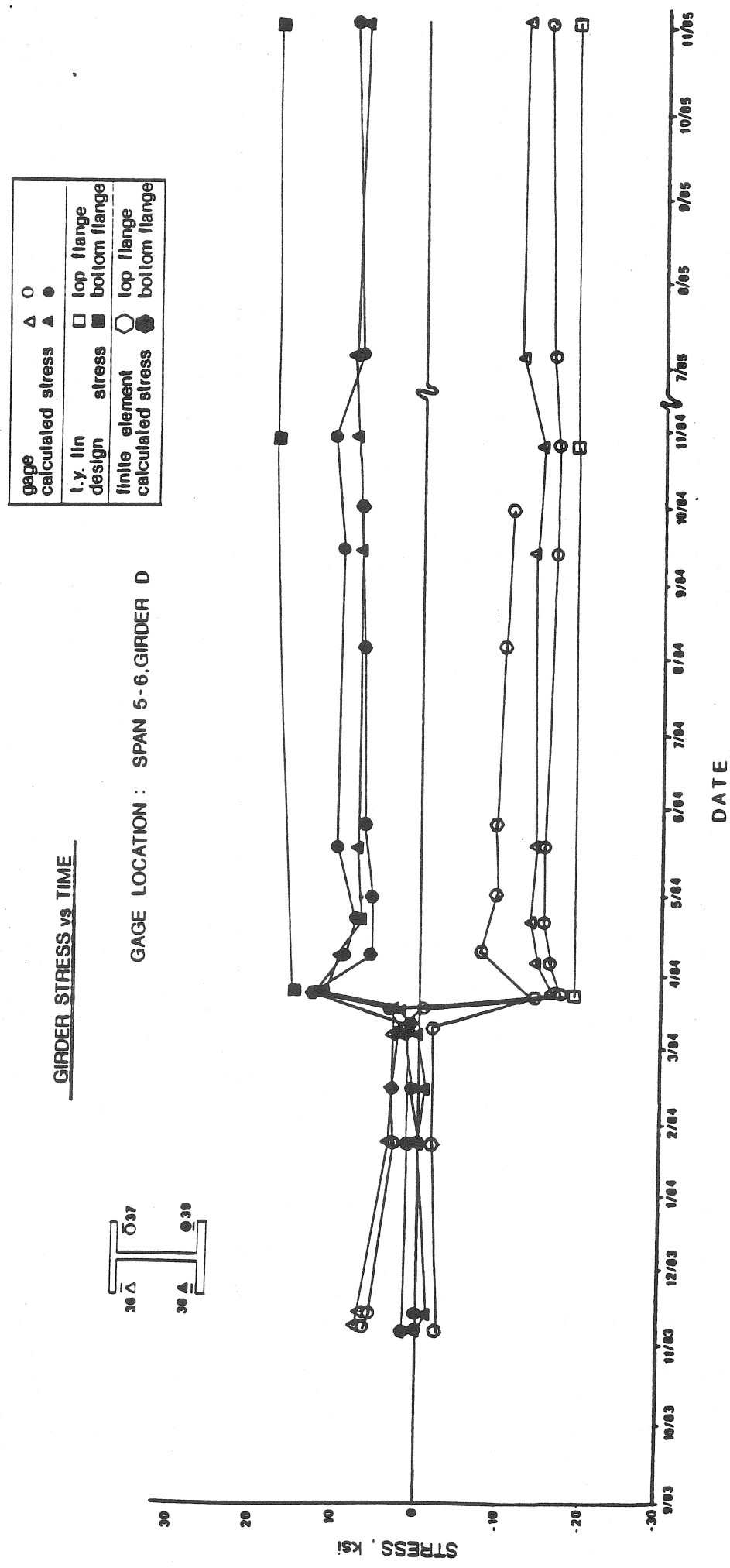


Figure 20

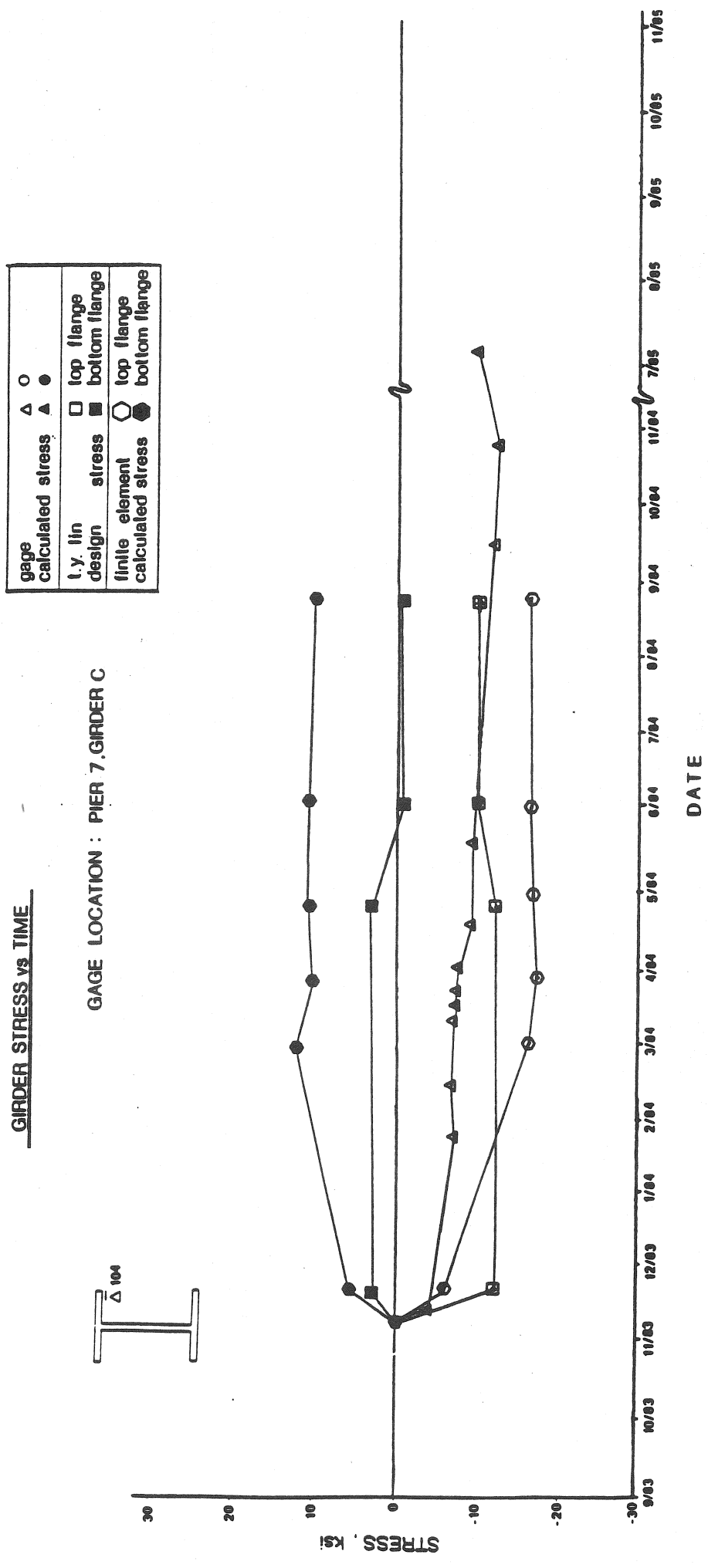


Figure 21

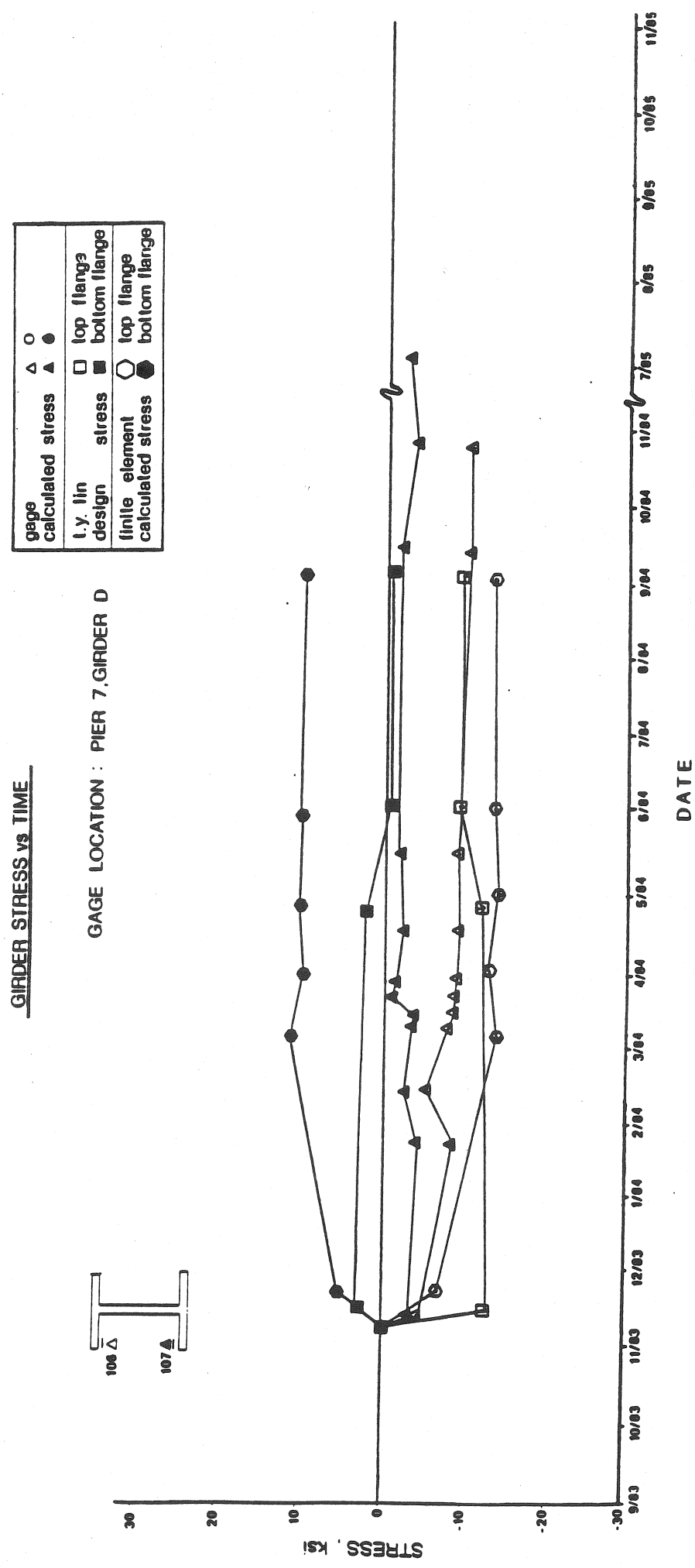


Figure 22

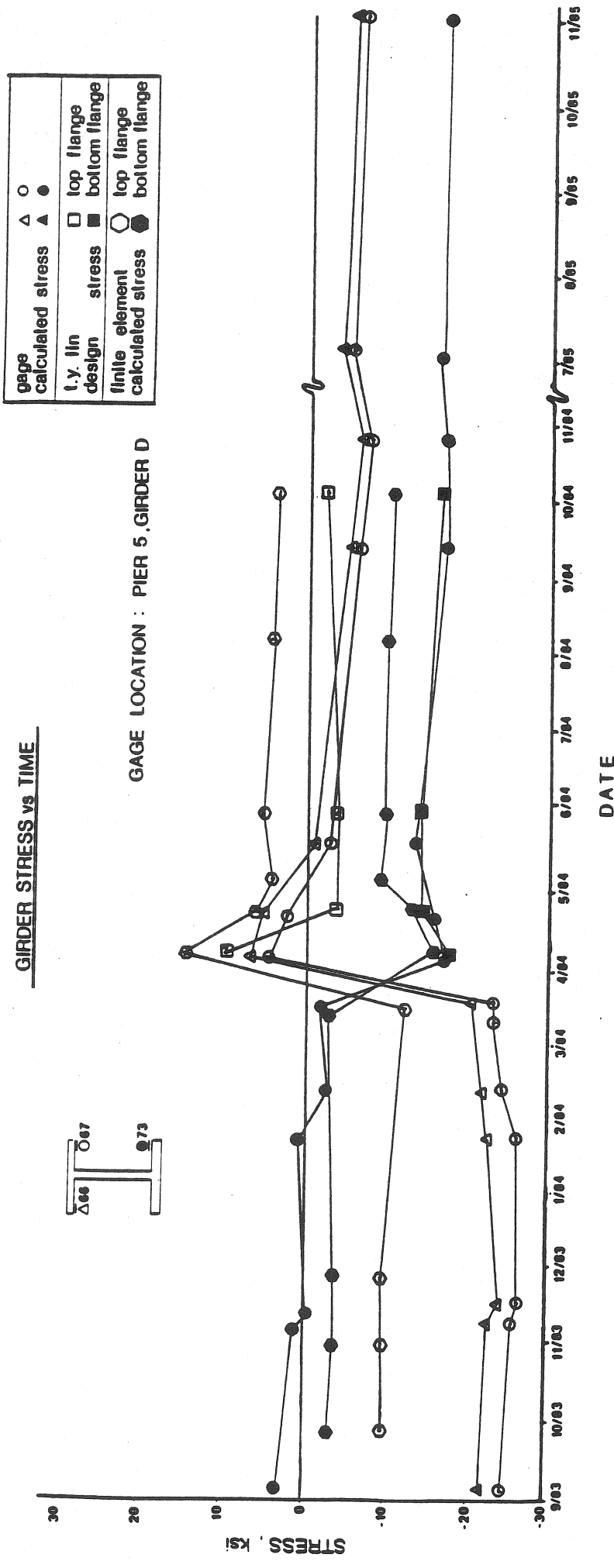


Figure 23

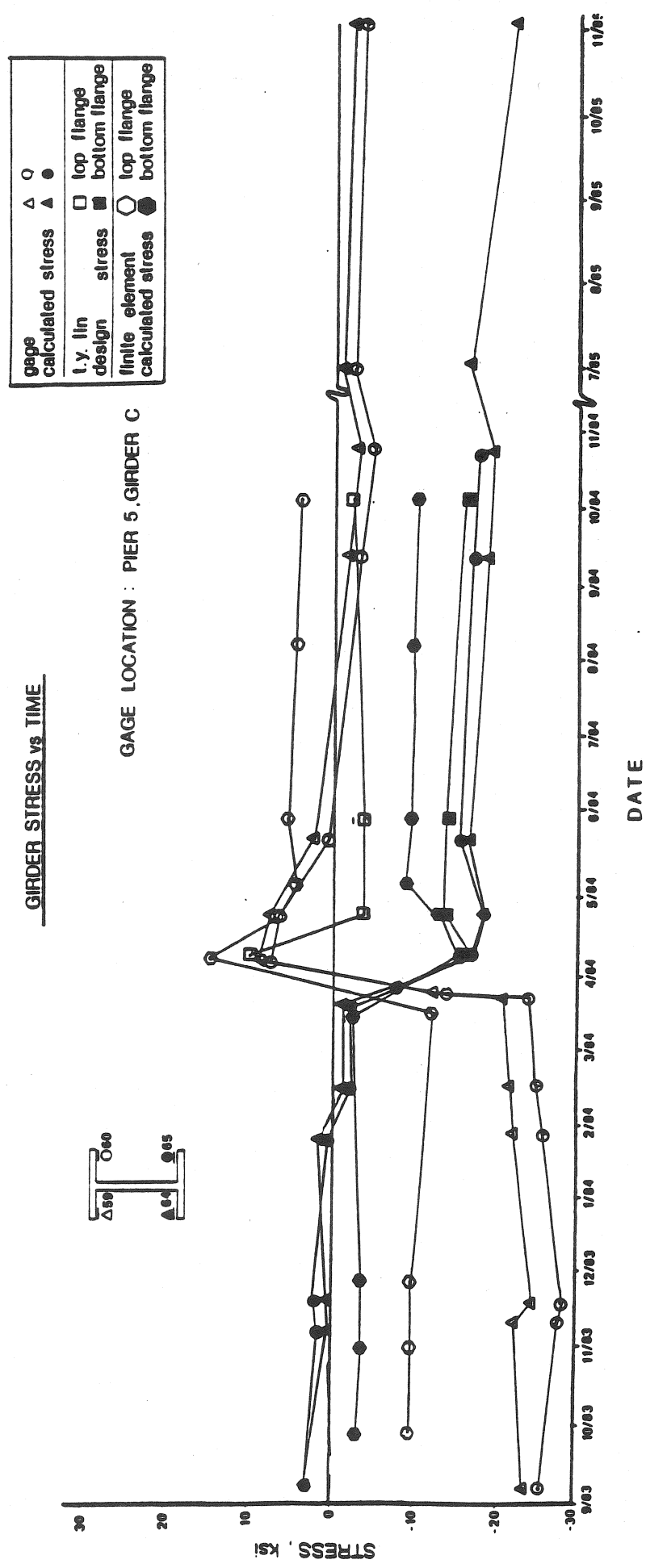


Figure 24

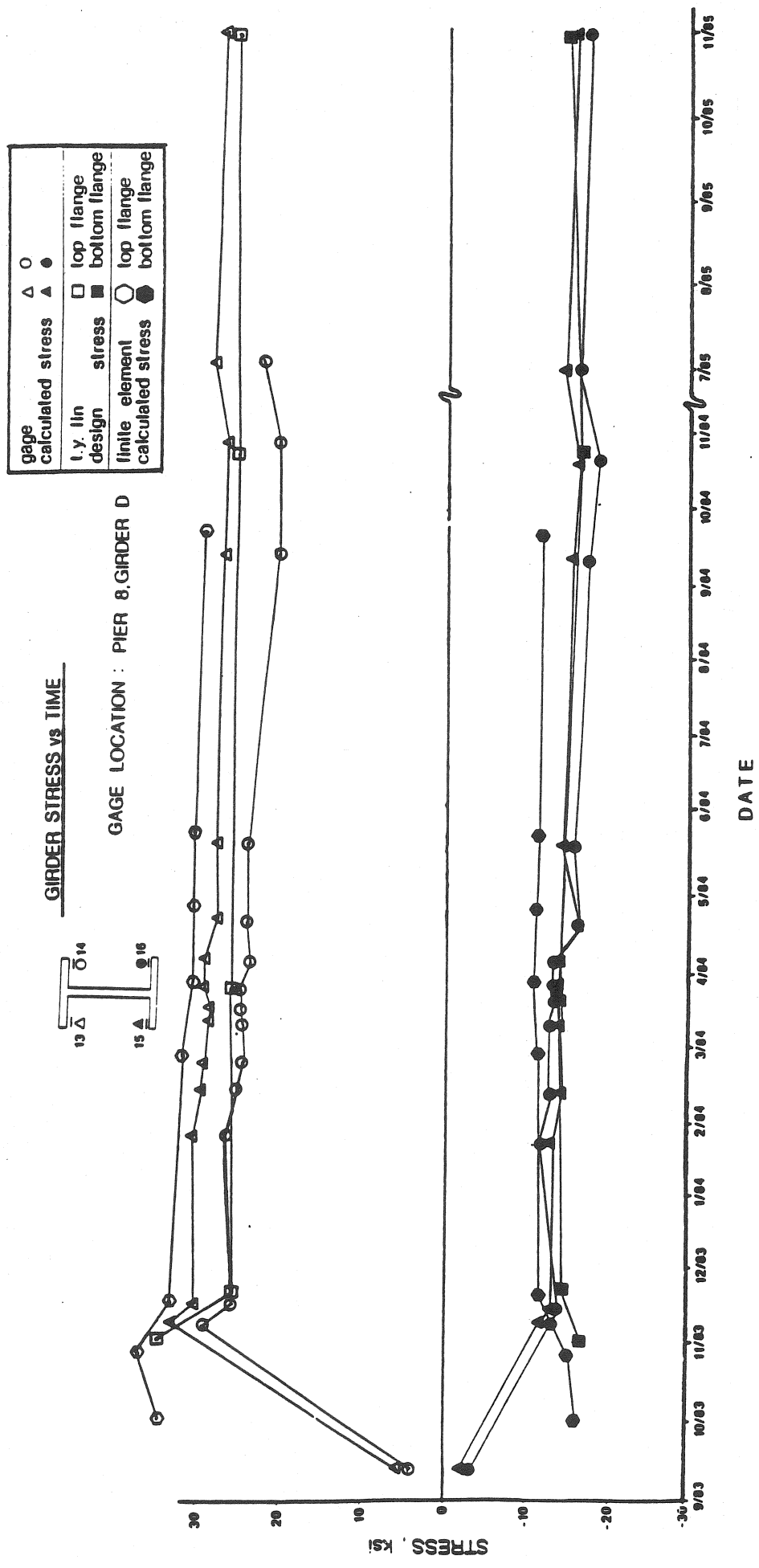


Figure 25

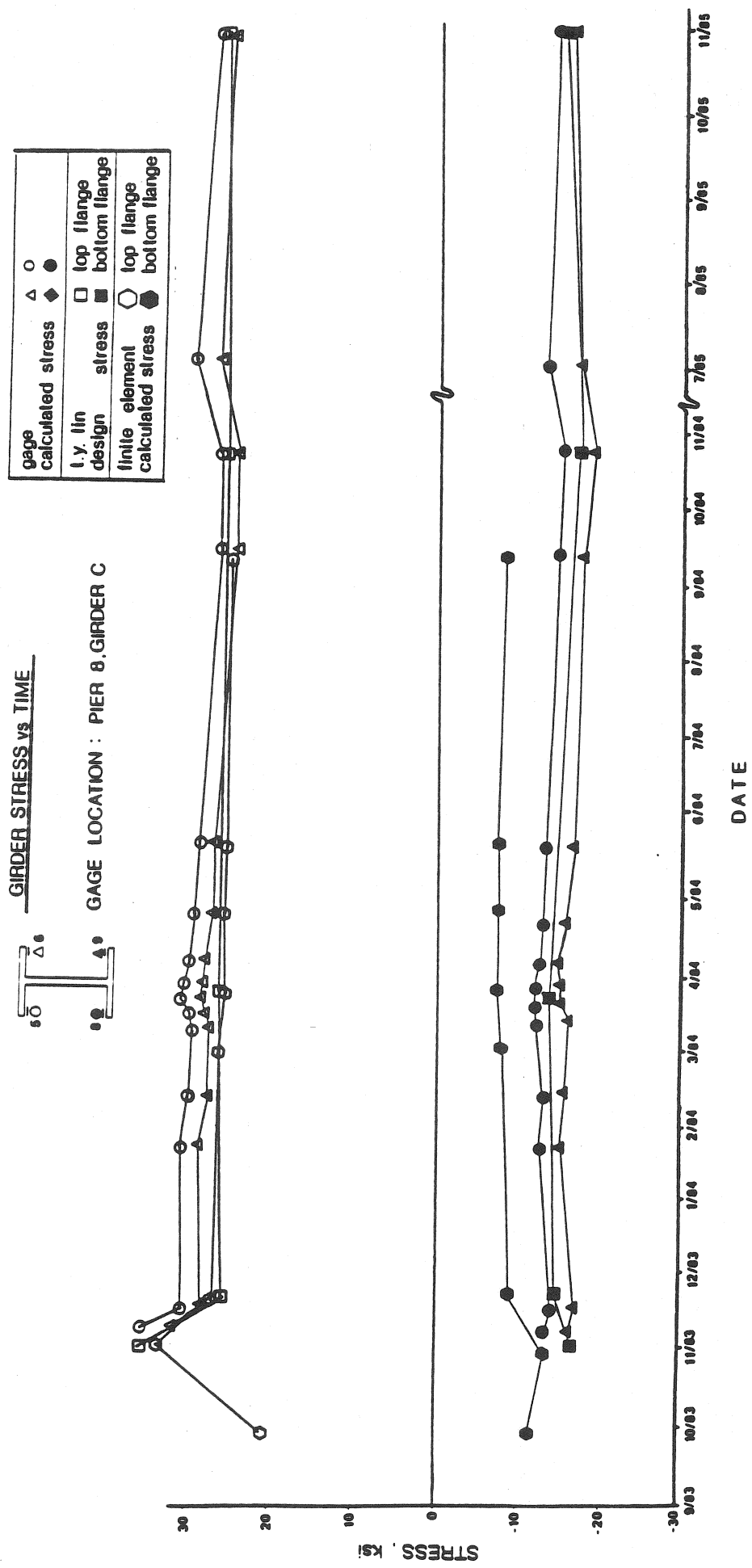


Figure 26

STRAIN DISTRIBUTION

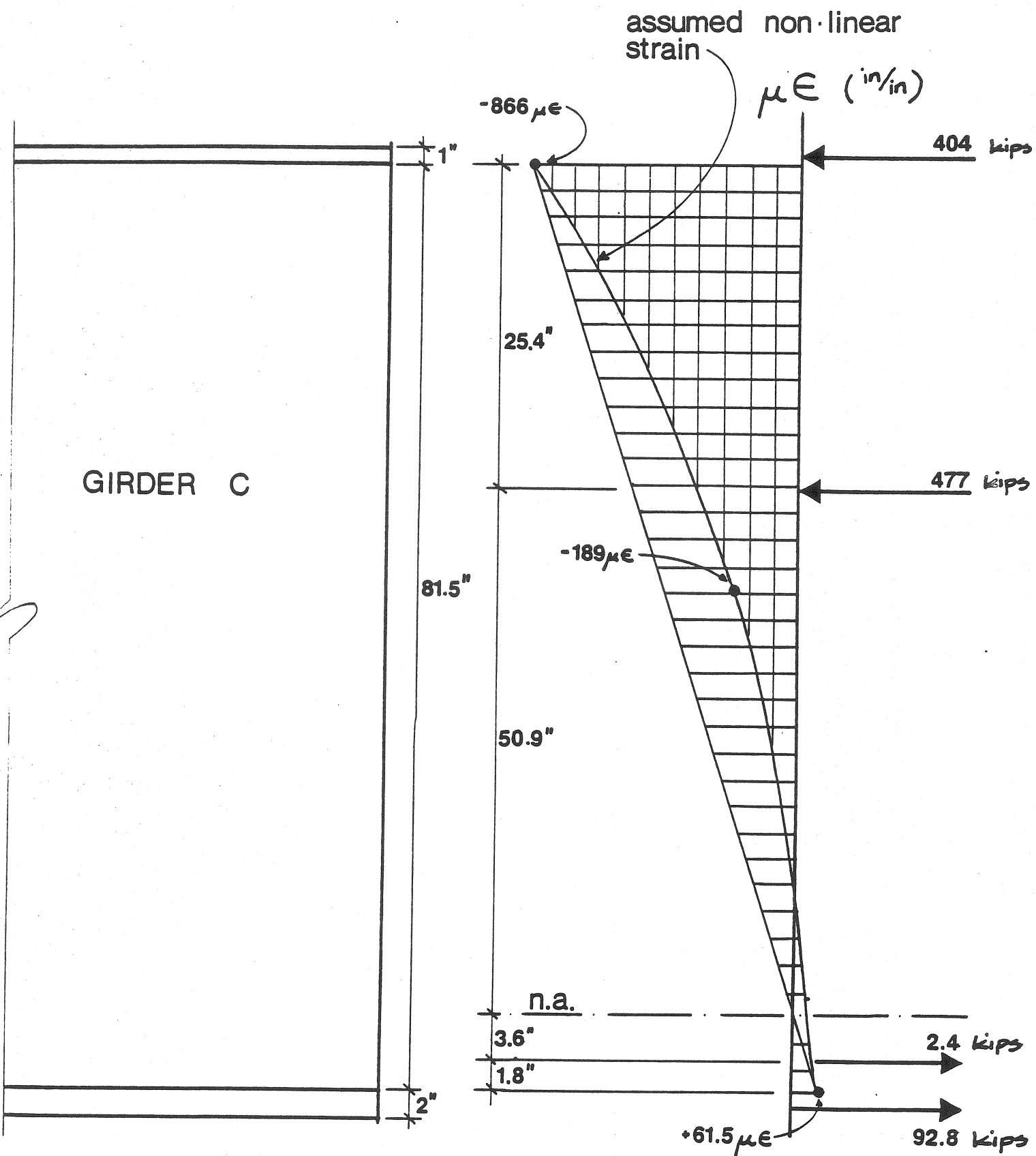


Figure 27

LIVE LOAD TEST: TRUCK LOCATIONS

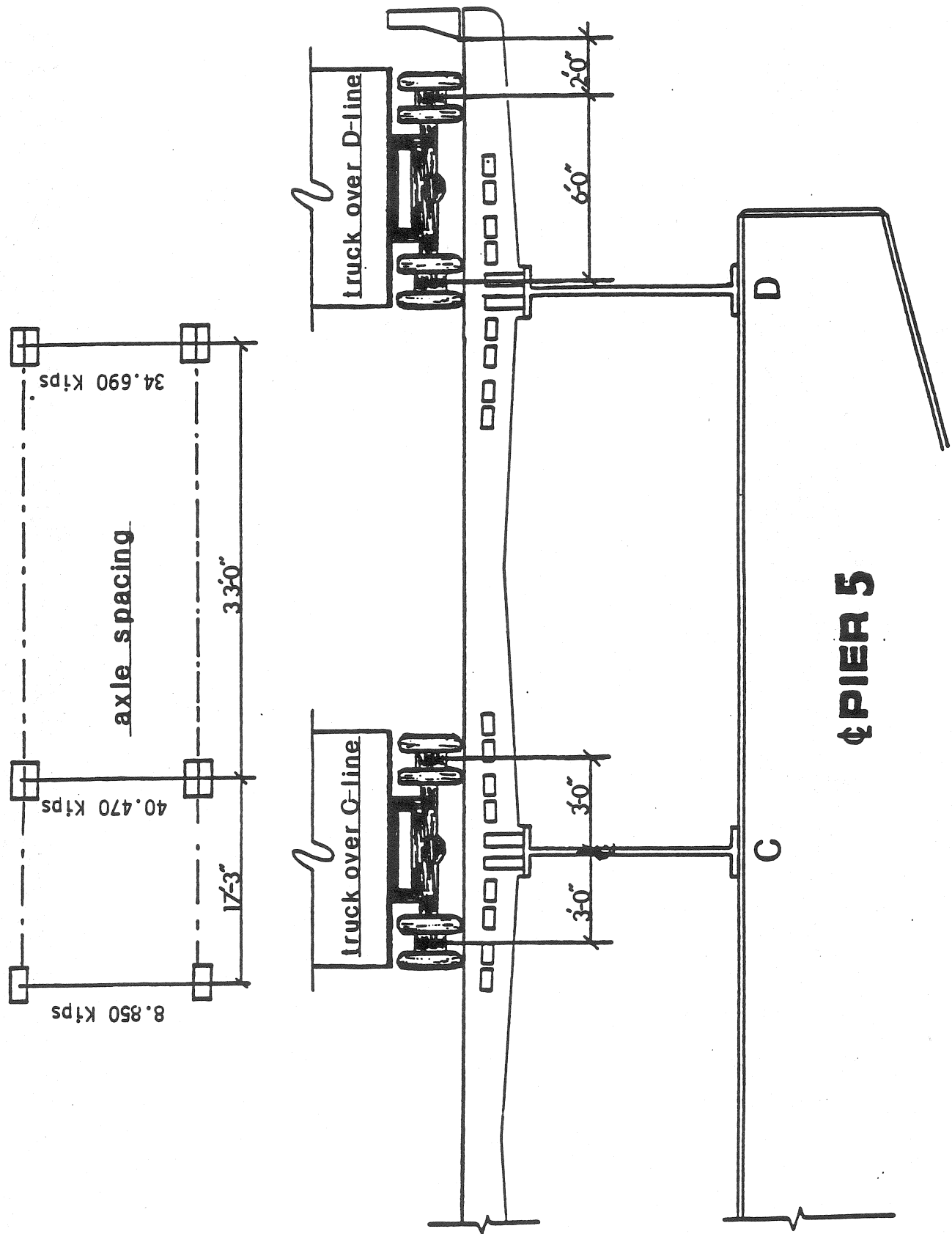


Figure 28

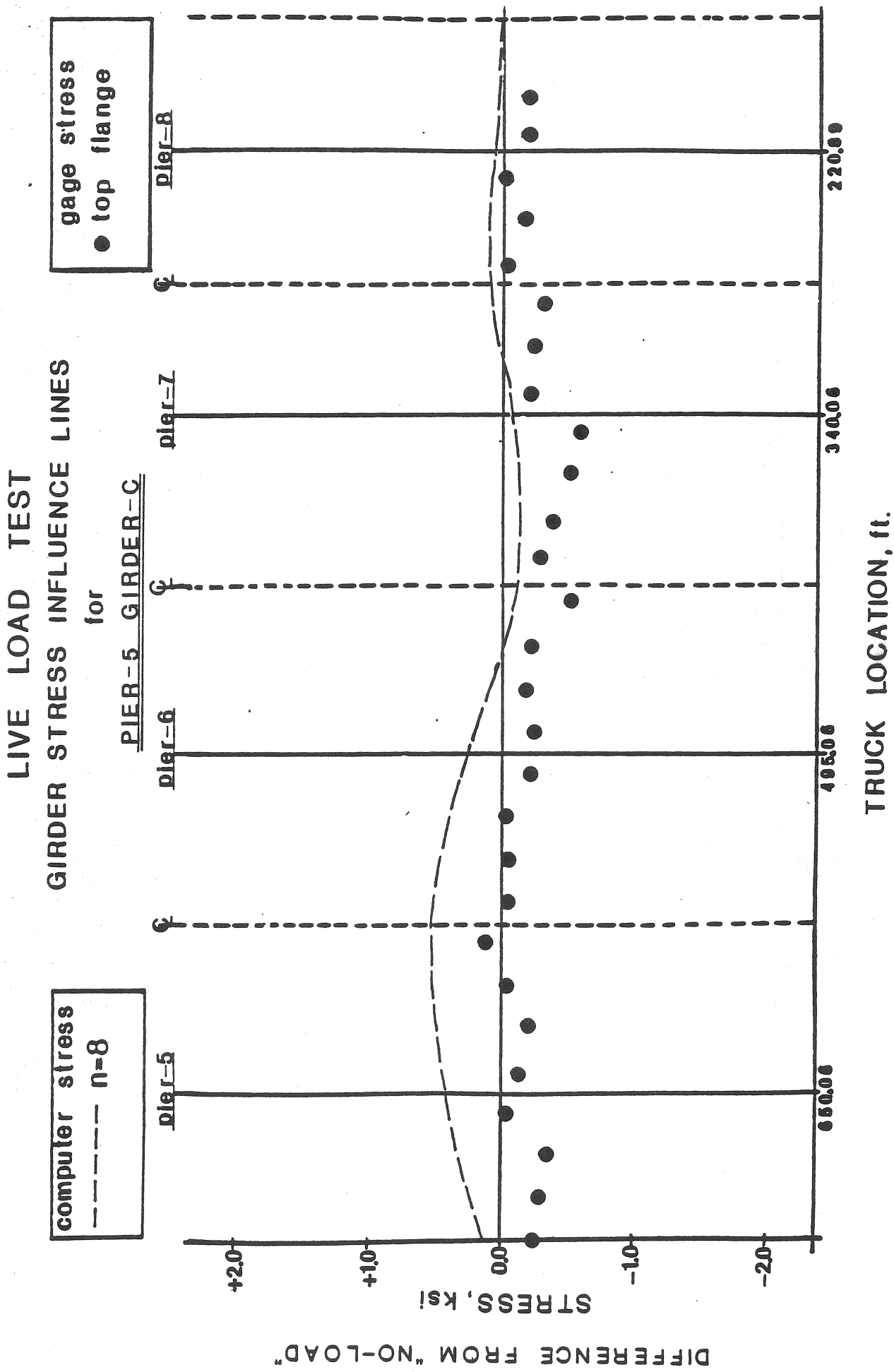


Figure 29

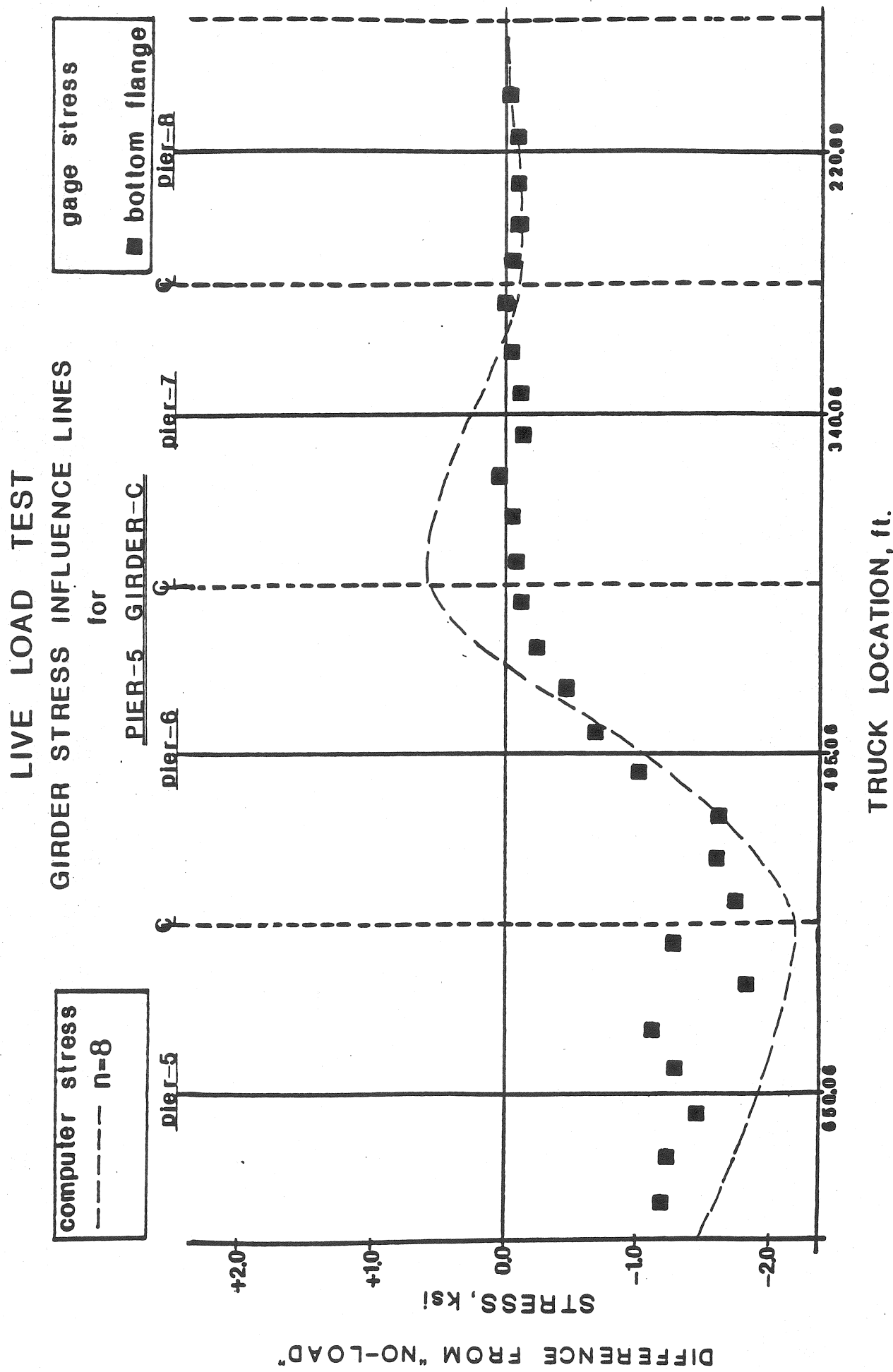
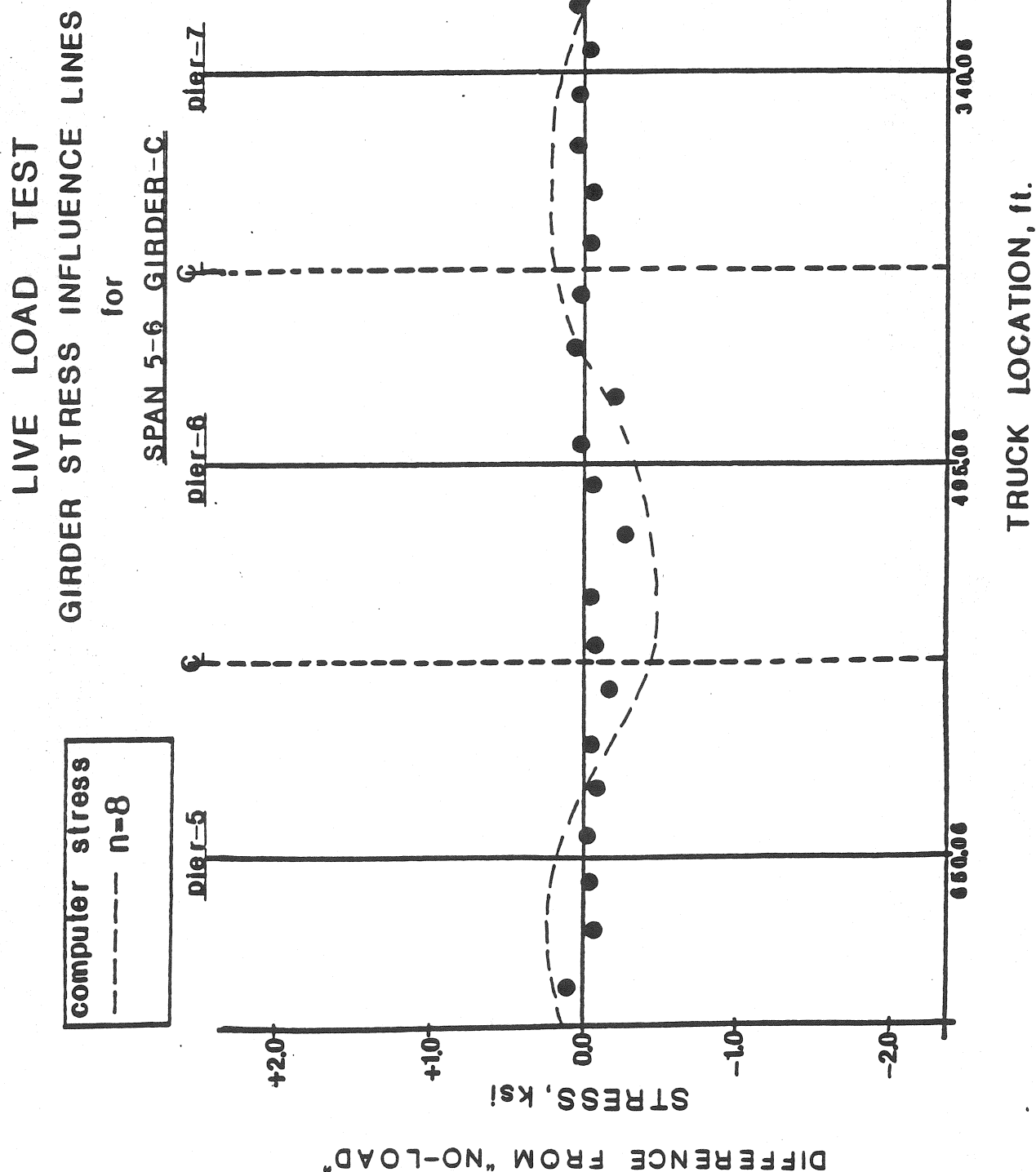


Figure 30



DIFFERENCE FROM "NO-LOAD"

Figure 31

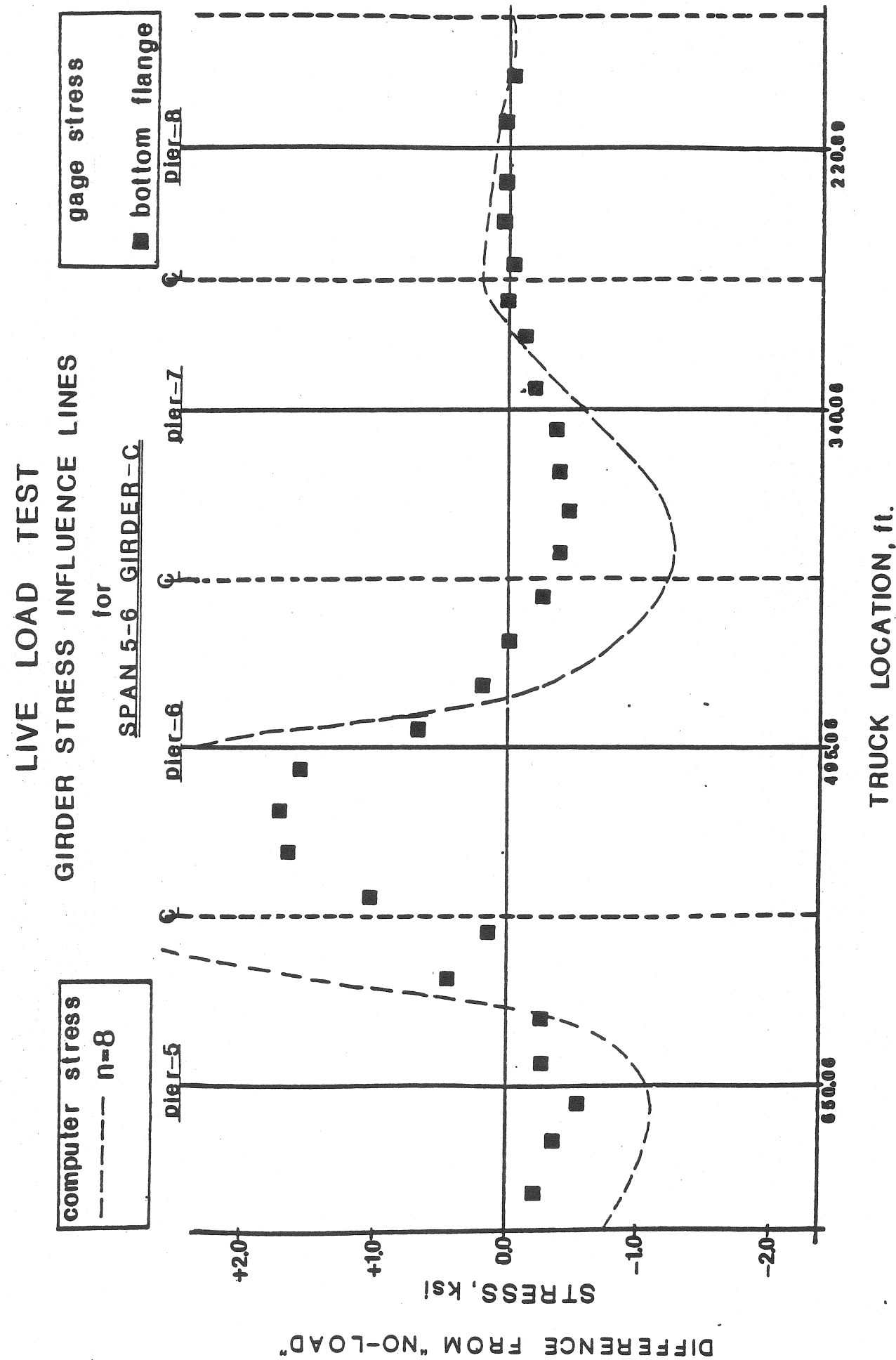


Figure 32

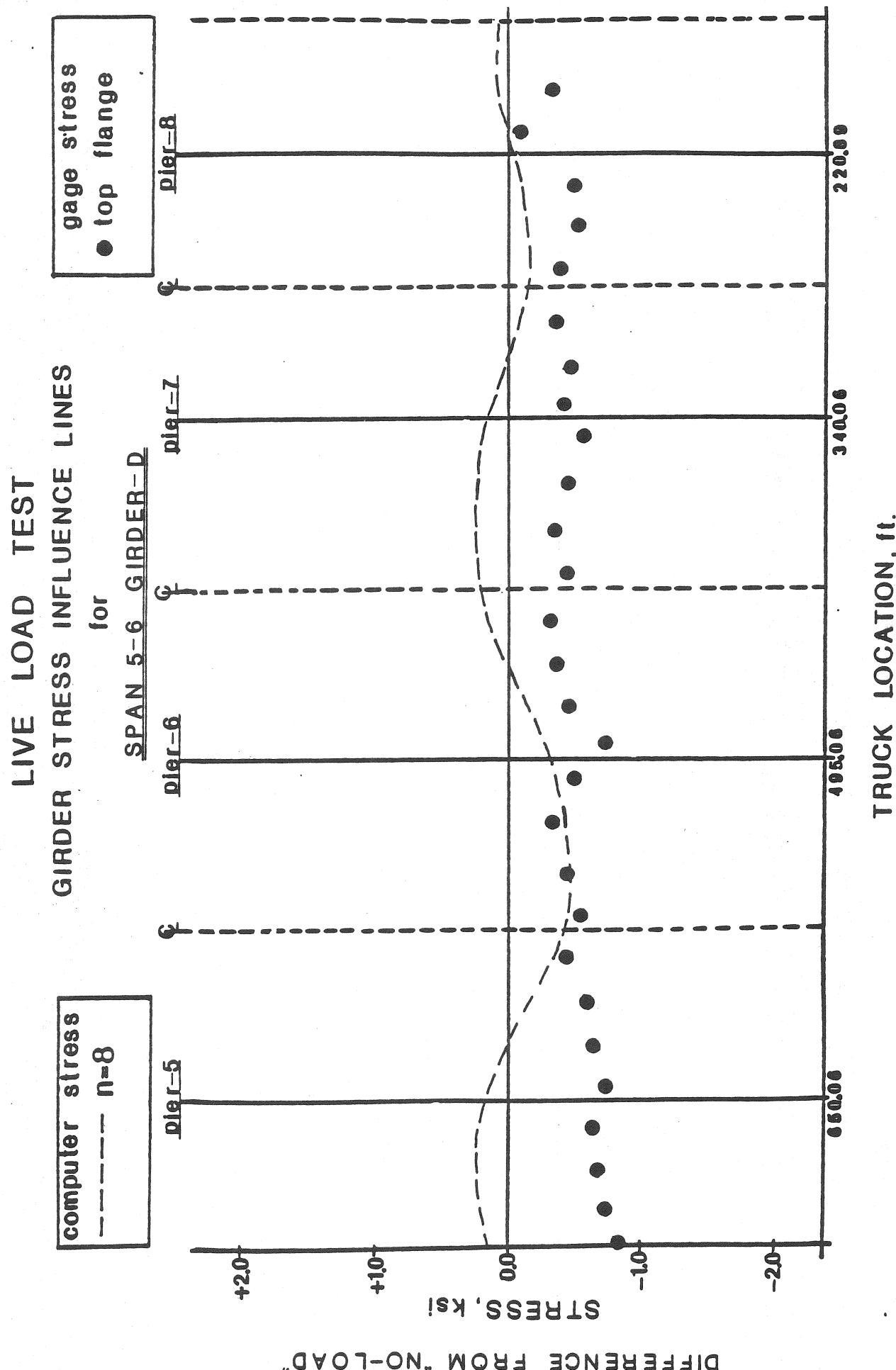


Figure 33

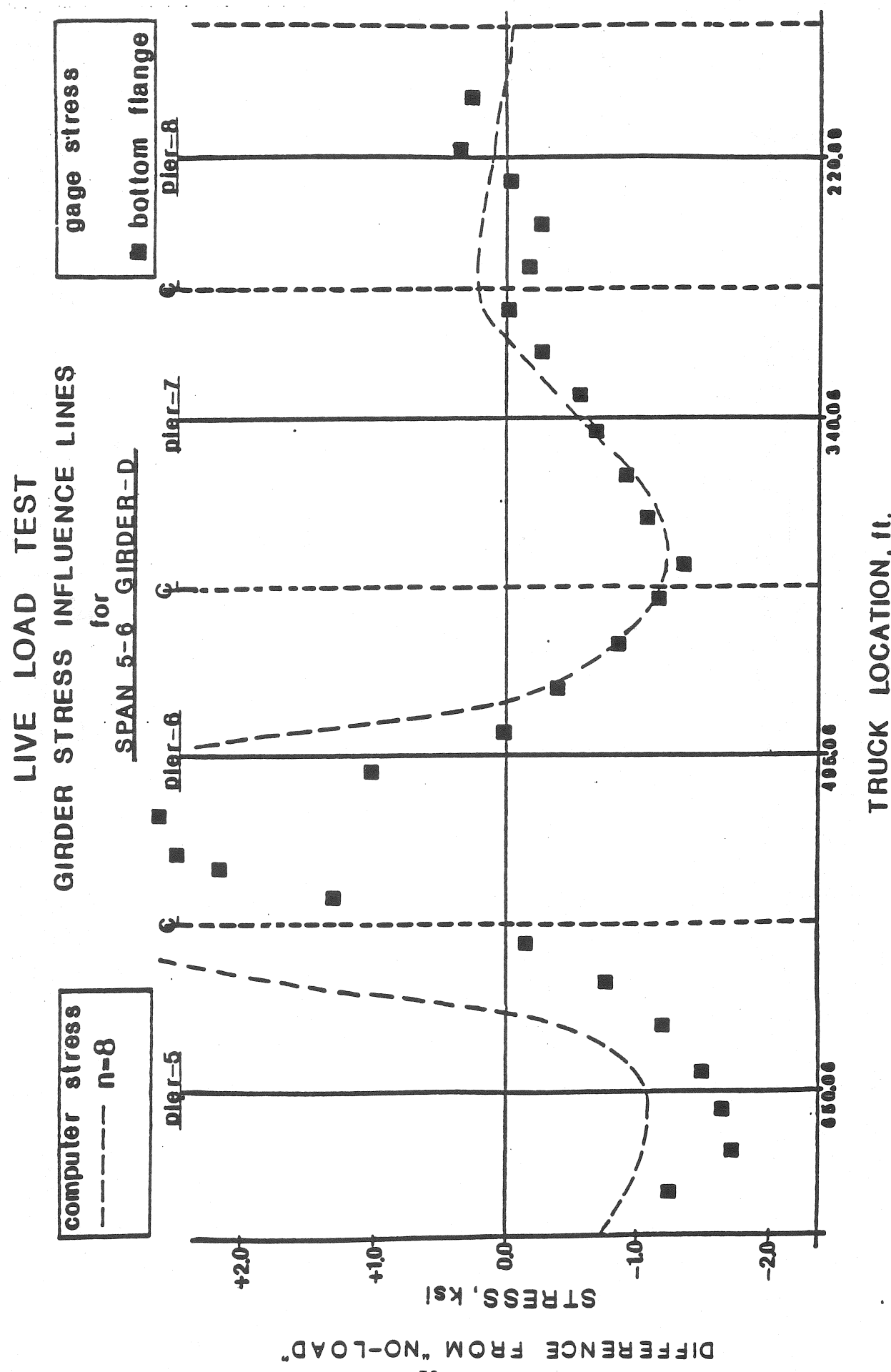


Figure 34

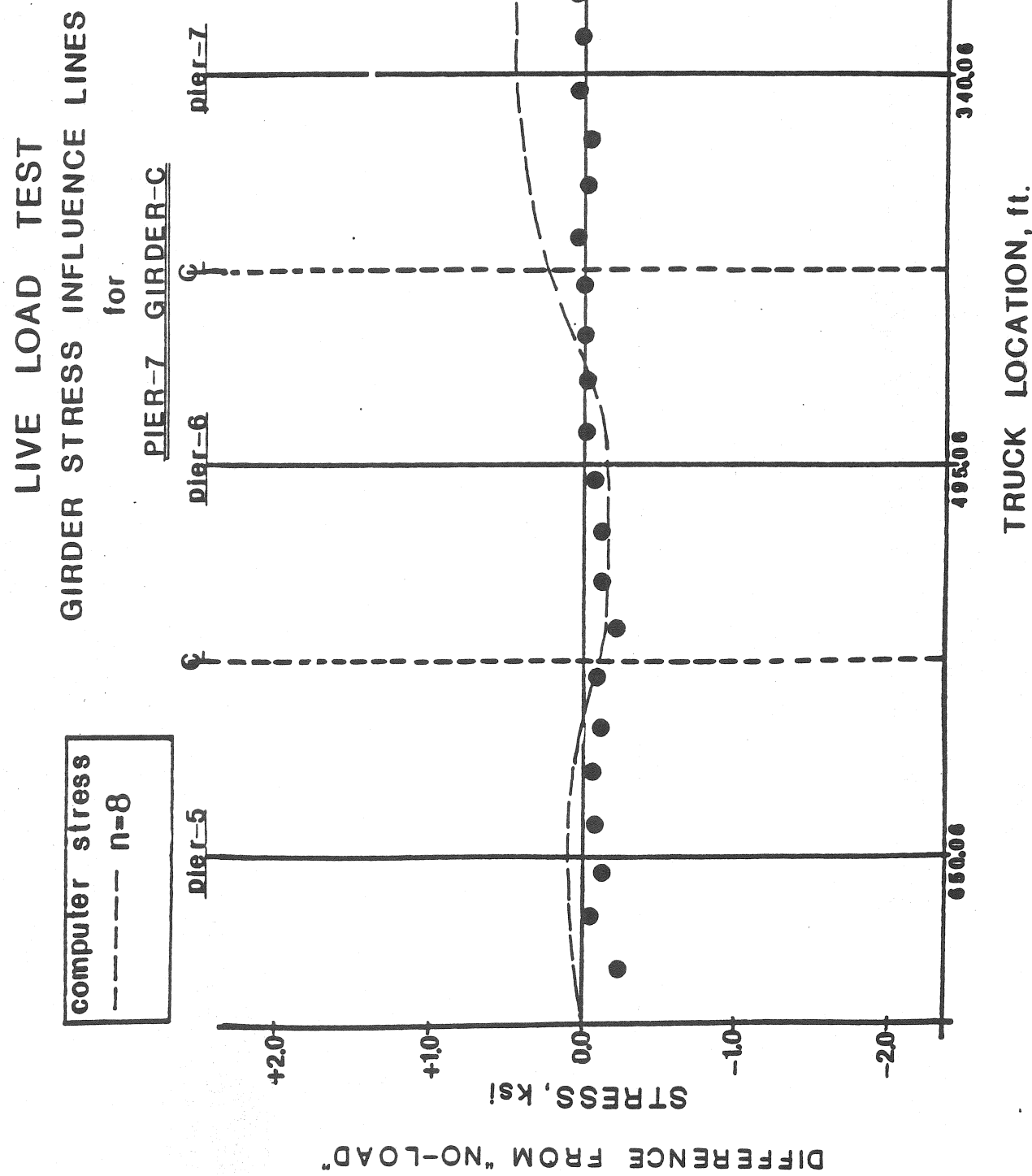
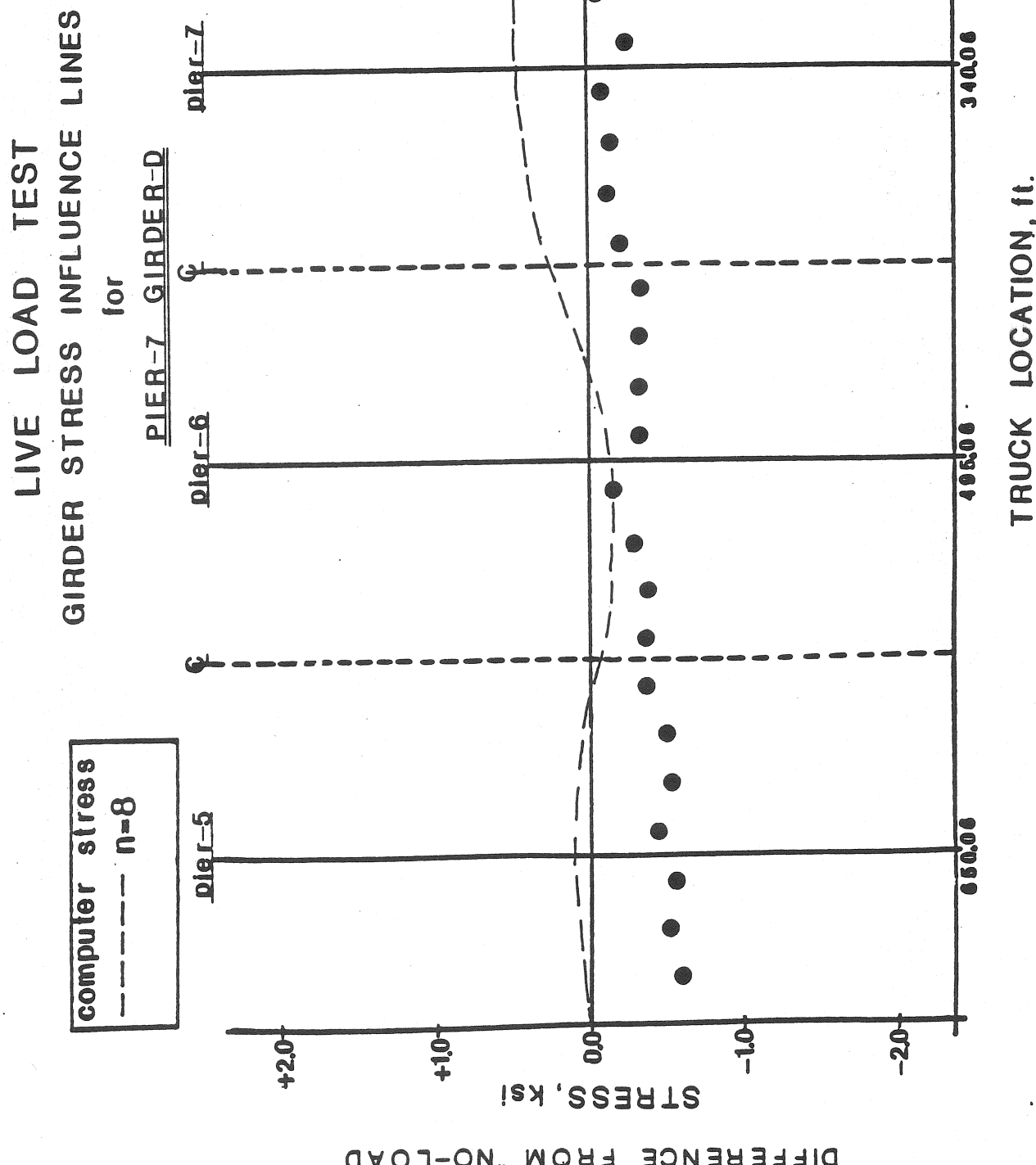


Figure 35



DIFFERENCE FROM "NO-LOAD"

Figure 36

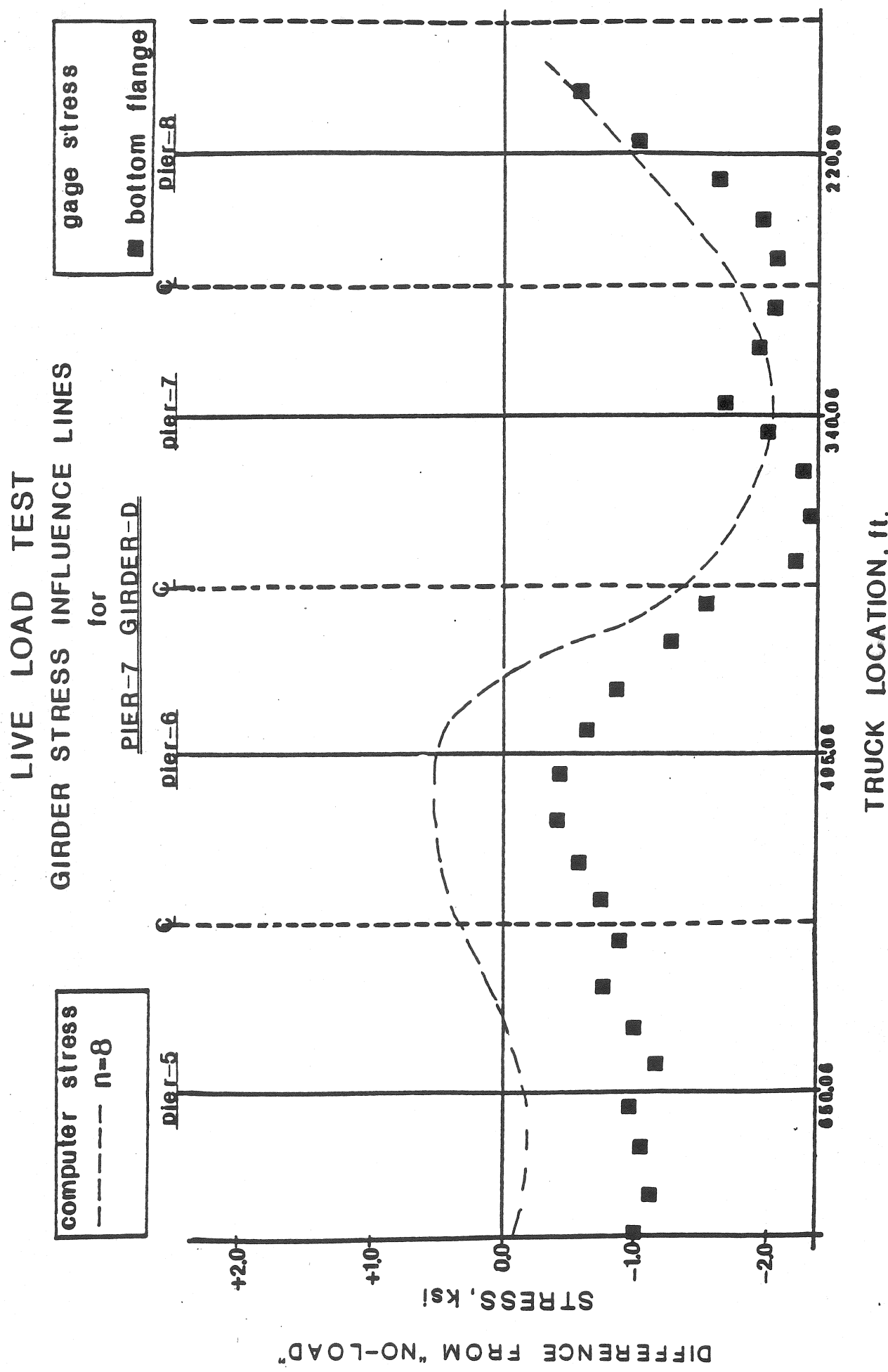


Figure 37

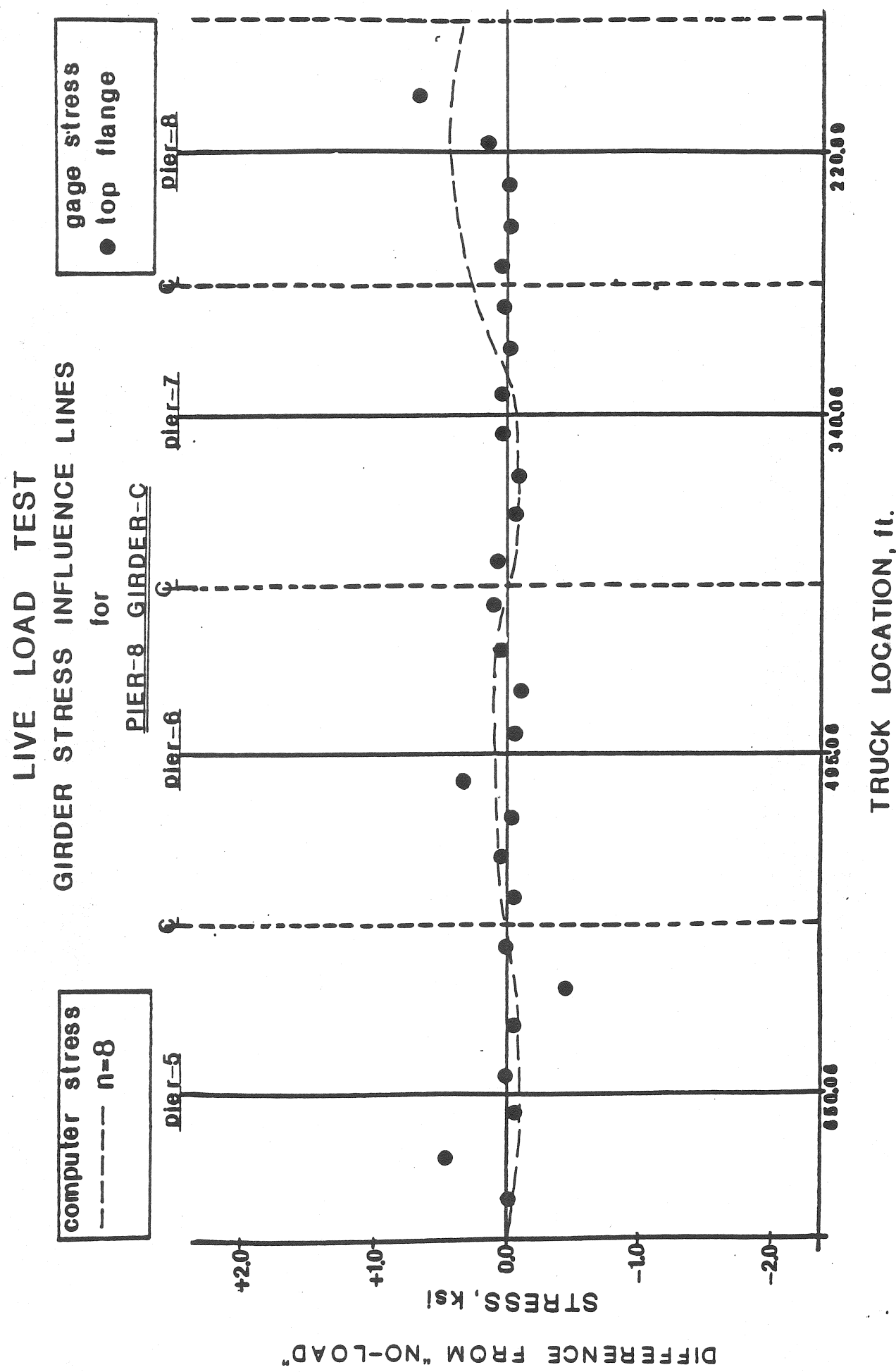


Figure 38

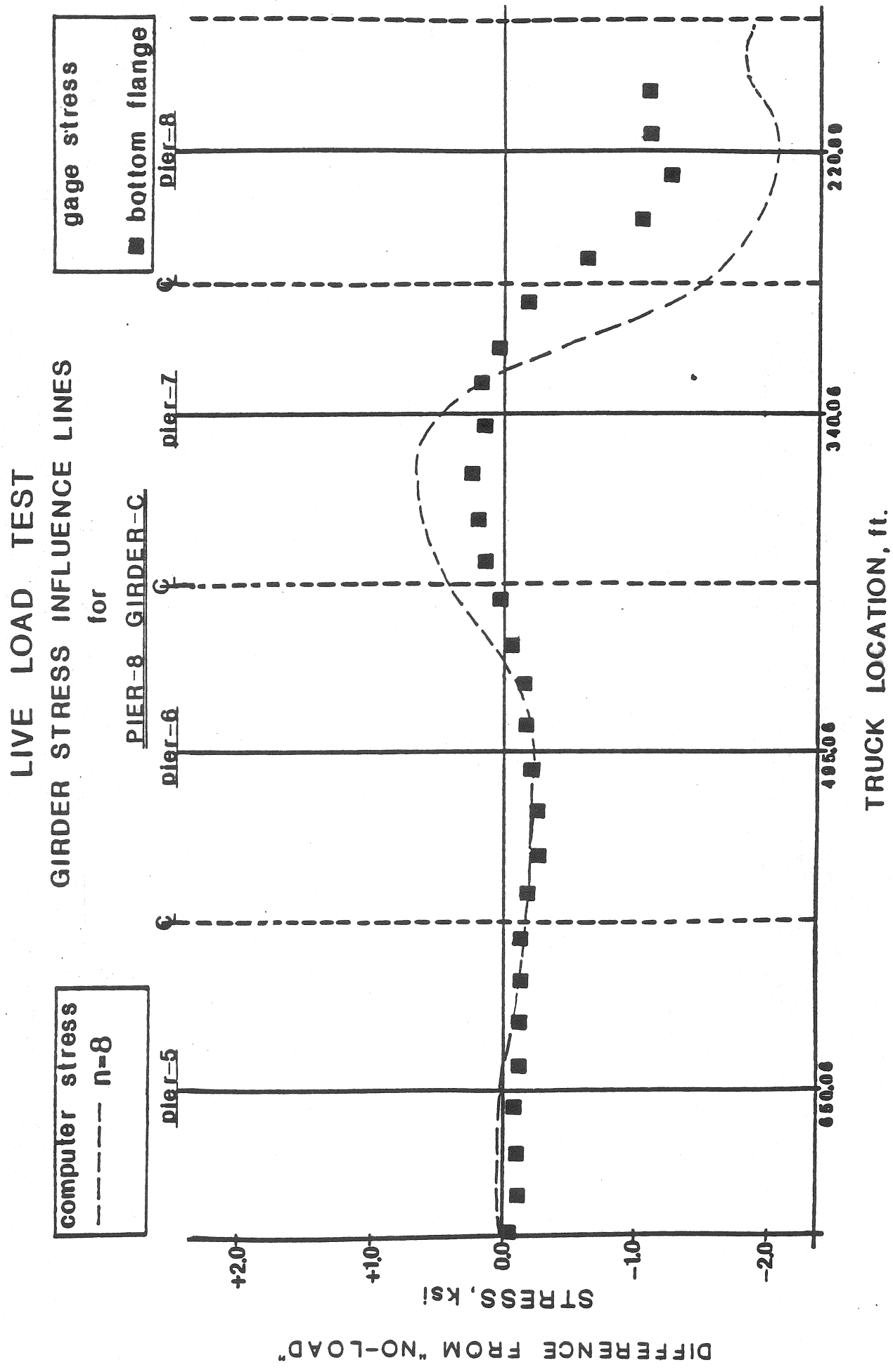


Figure 39

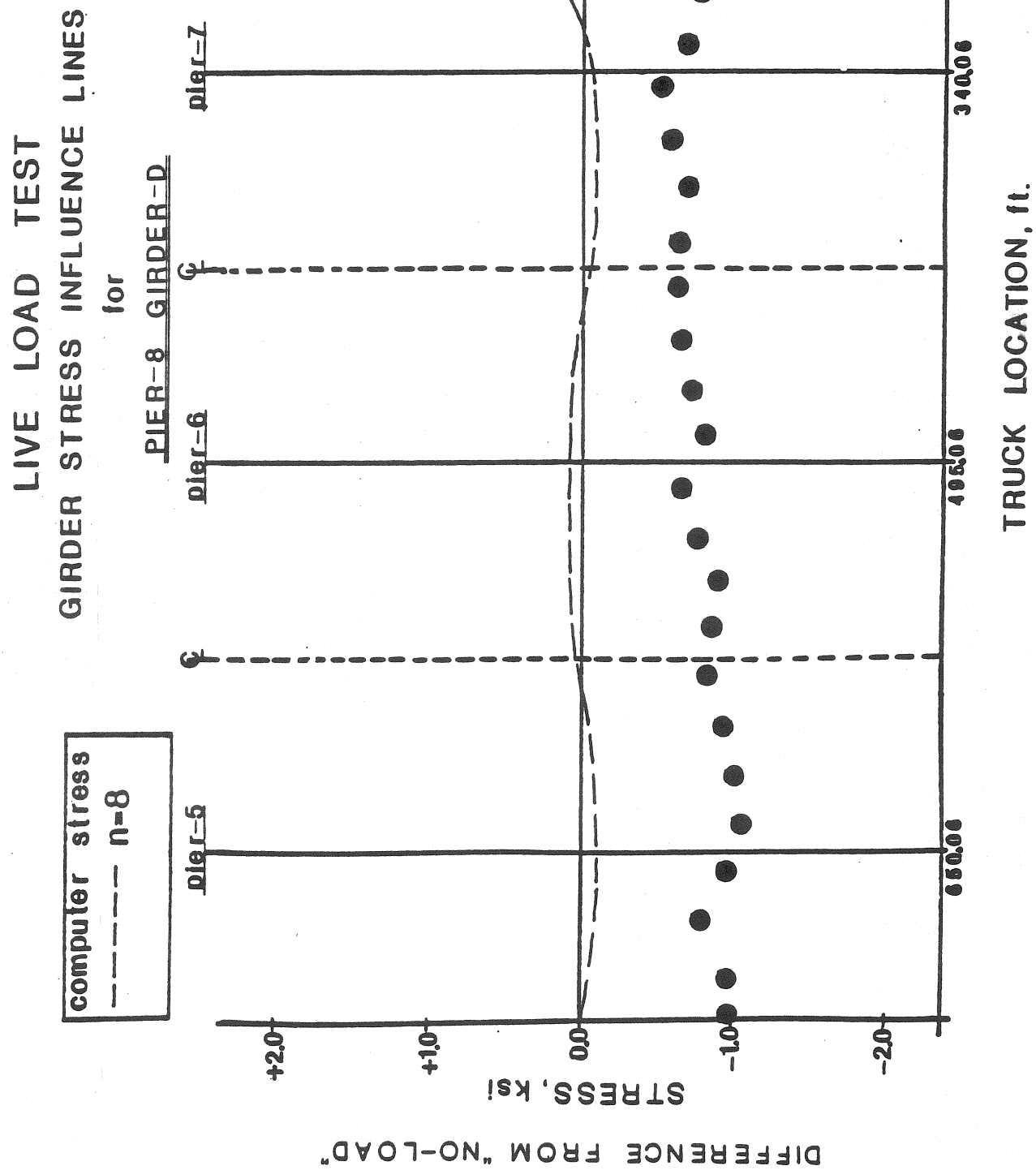


Figure 40

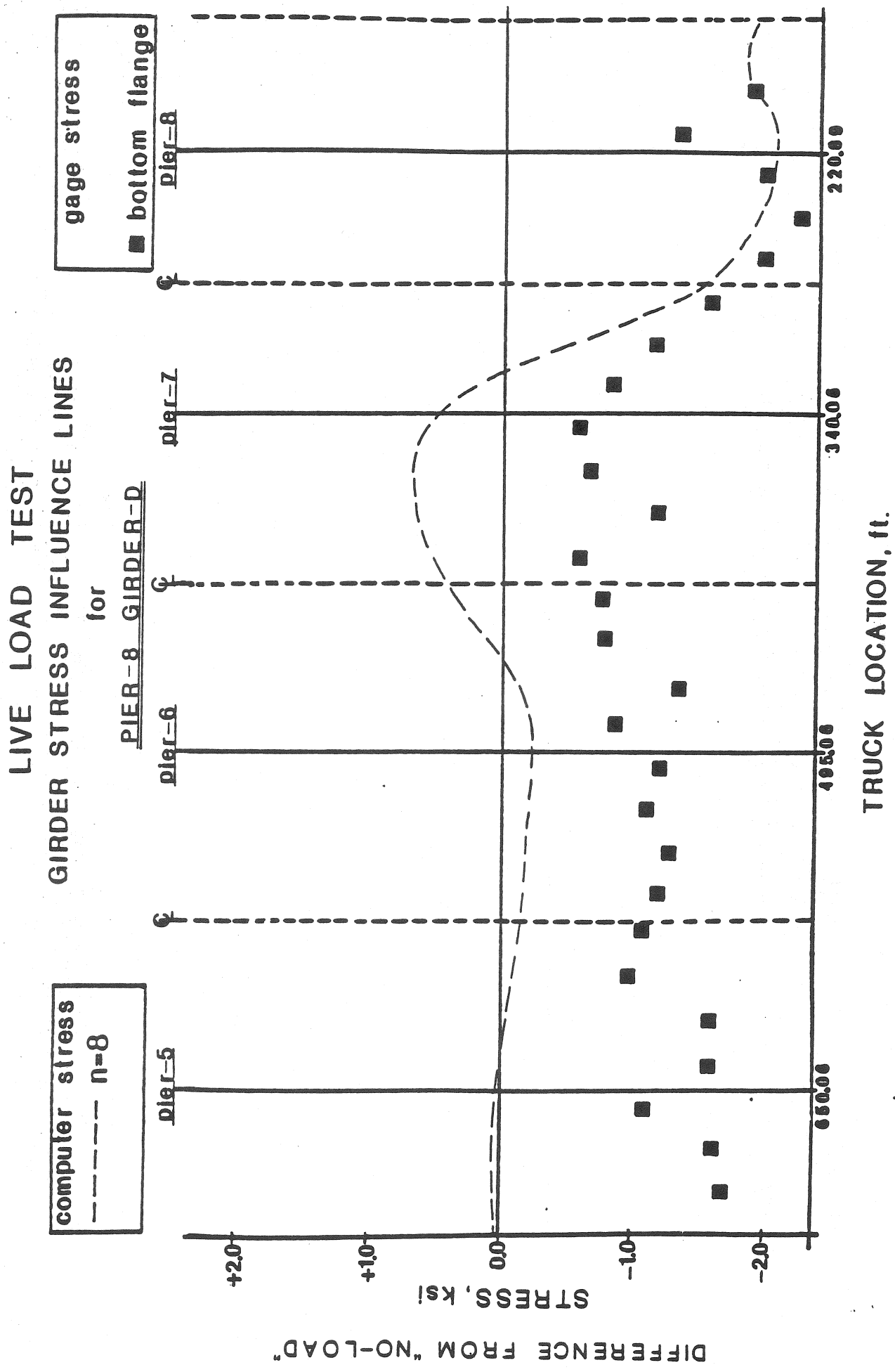


Figure 41

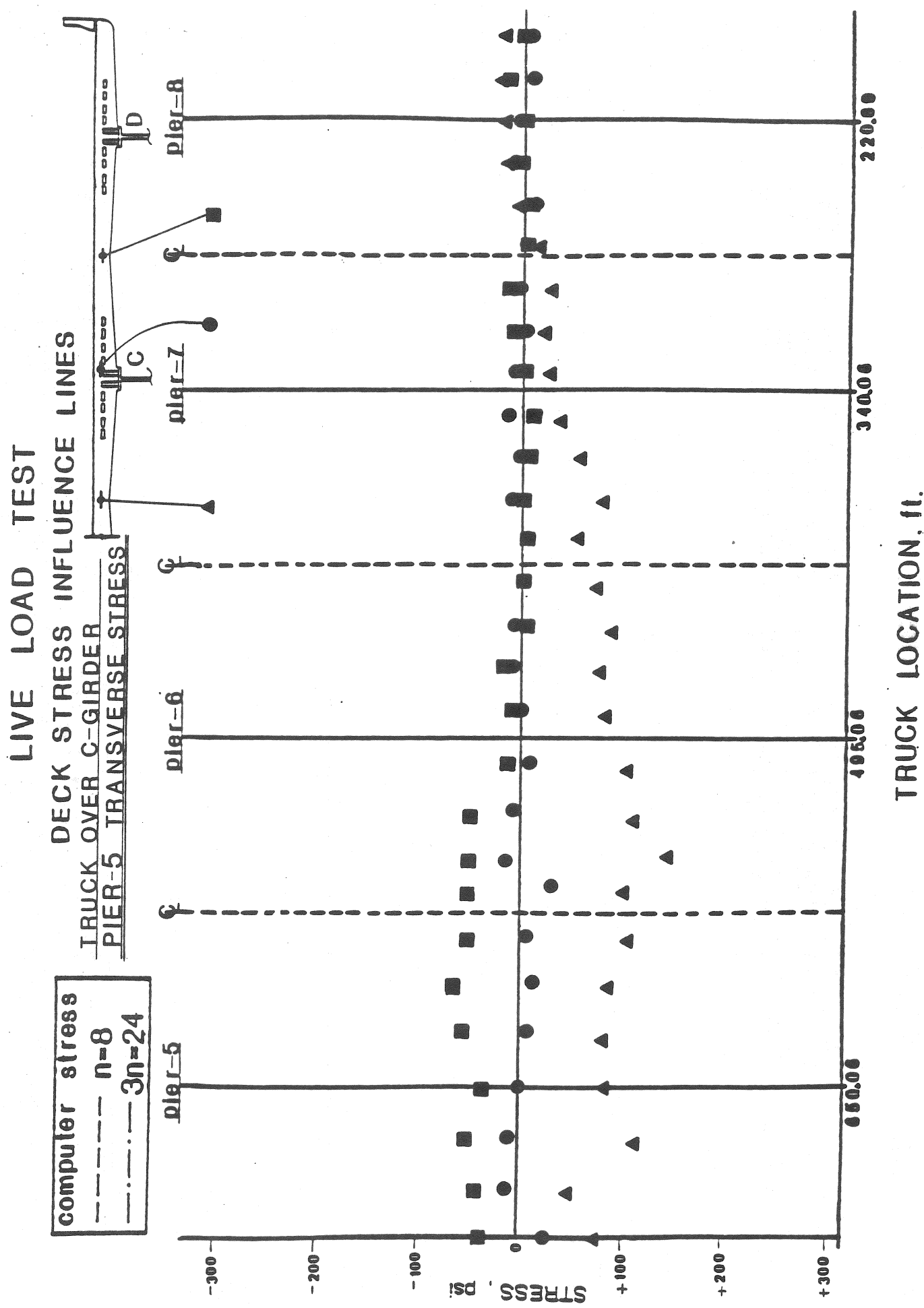


Figure 42

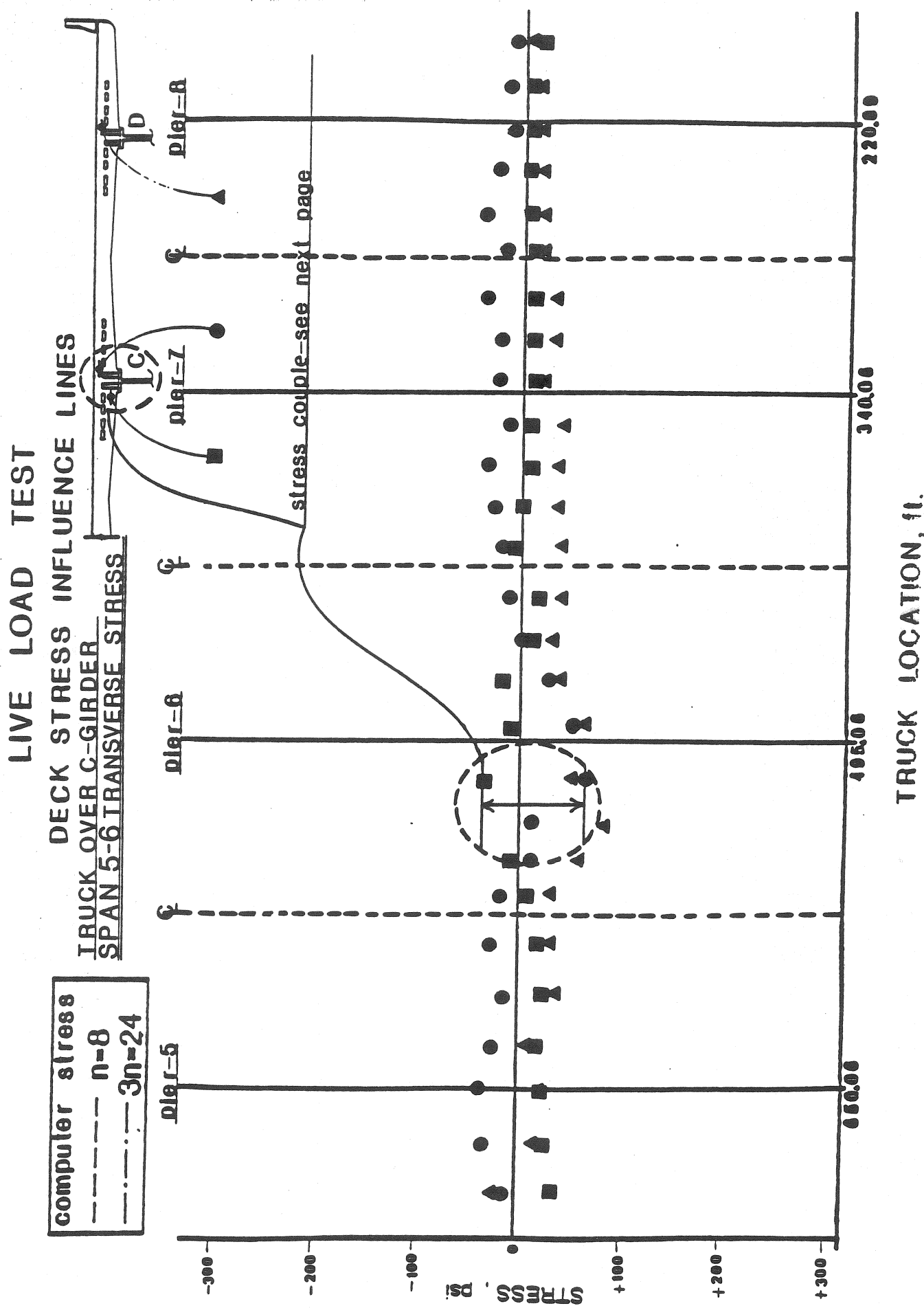


Figure 43

SPAN 5-6
TRANSVERSE DECK STRESS
STRESS COUPLE

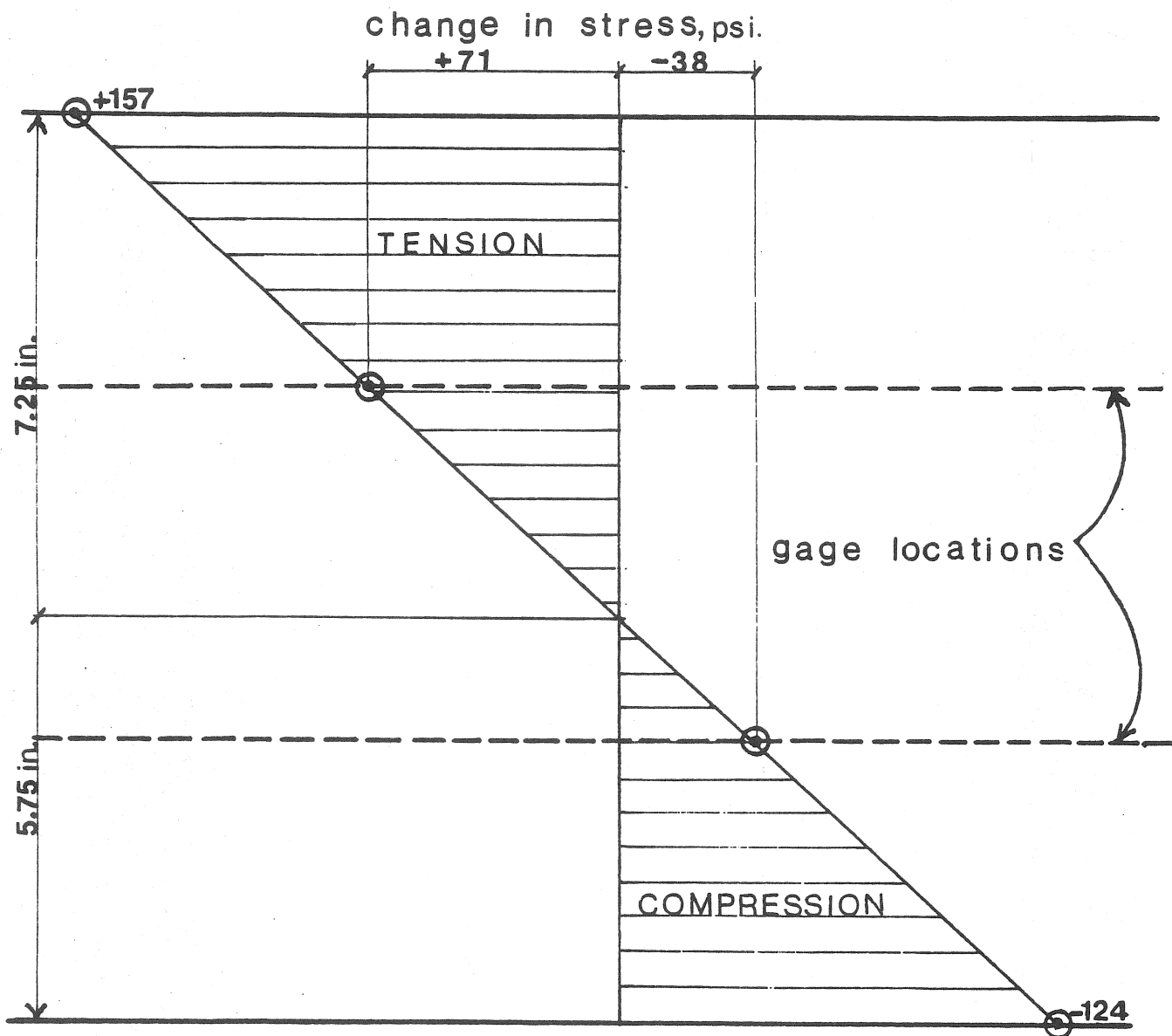


Figure 44

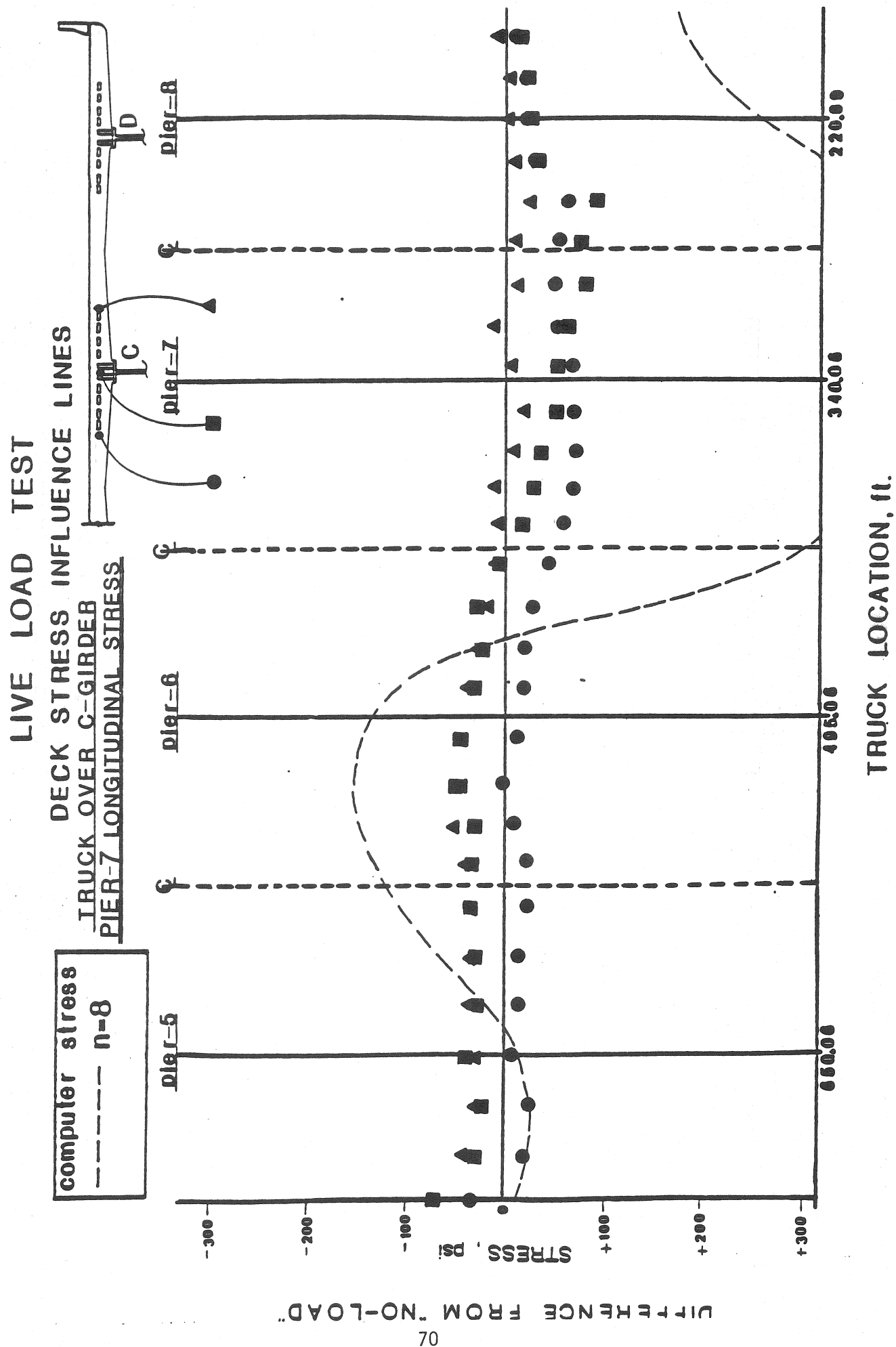


Figure 45

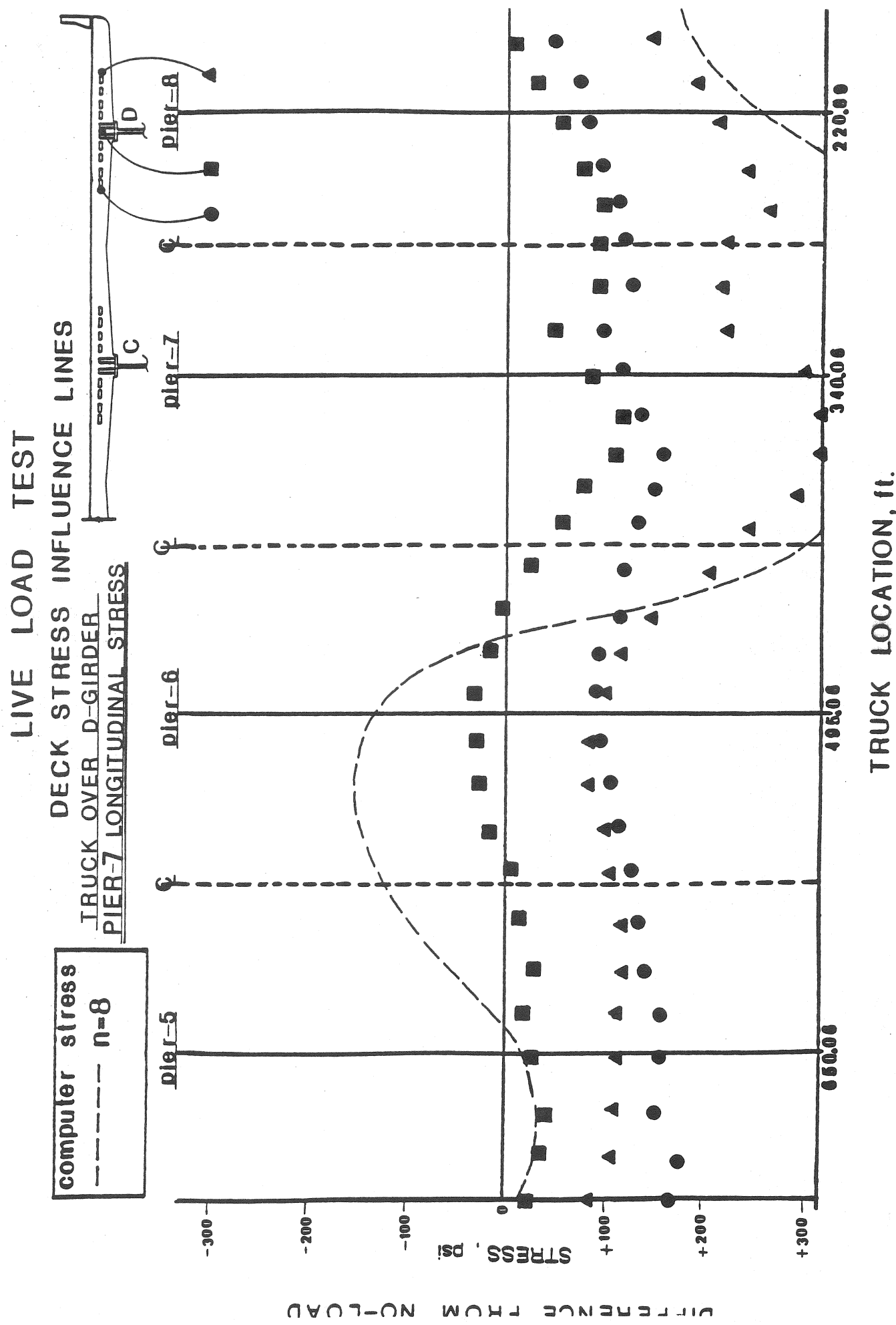


Figure 46

